NASA MEMO 1-20-59A

NASA

MEMORANDUM

BOUNDARY-LAYER TRANSITION ON HOLLOW CYLINDERS IN SUPERSONIC FREE FLIGHT AS AFFECTED BY MACH NUMBER AND A SCREWTHREAD TYPE OF SURFACE ROUGHNESS

By Carlton S. James

Ames Research Center
Moffett Field, Calif.

NATIONAL AERONAUTICS AND SPACE ADMINISTRATION
WASHINGTON
February 1959

NATIONAL AERONAUTICS AND SPACE ADMINISTRATION

MEMORANDUM 1-20-59A

BOUNDARY-LAYER TRANSITION ON HOLLOW CYLINDERS IN SUPERSONIC FREE FLIGHT AS AFFECTED BY MACH NUMBER AND A SCREWTHREAD TYPE OF SURFACE ROUGHNESS

By Carlton S. James

SUMMARY

The effects of Mach number and surface-roughness variation on boundary-layer transition were studied using fin-stabilized hollow-tube models in free flight. The tests were conducted over the Mach number range from 2.8 to 7 at a nominally constant unit Reynolds number of 3 million per inch, and with heat transfer to the model surface. A screwthread type of distributed two-dimensional roughness was used. Nominal thread heights varied from 100 microinches to 2100 microinches.

Transition Reynolds number was found to increase with increasing Mach number at a rate depending simultaneously on Mach number and roughness height. The laminar boundary layer was found to tolerate increasing amounts of roughness as Mach number increased. For a given Mach number an optimum roughness height was found which gave a maximum laminar run greater than was obtained with a smooth surface.

INTRODUCTION

The advantages of a laminar boundary layer, in terms of reduced aerodynamic heating and skin friction, are well known. These advantages have assumed increasing importance to the designer as flight speeds have increased. It is of interest, therefore, to examine the effect of speed itself on boundary-layer transition. At present there is little information available on this subject for negligible stream turbulence and for flight Reynolds numbers. Some wind-tunnel tests (refs. 1 and 2) have indicated a decrease in the Reynolds number of transition with increasing Mach number in the Mach number range of approximately 1.5 to 3.5. Other wind-tunnel tests and some flight tests (ref. 3) have indicated an increase in the Reynolds number of transition with increasing Mach number in the same range. A few relatively recent investigations (refs. 4 and 5) have shown a tendency of transition Reynolds number to decrease as Mach number is increased in this range, but to increase with a further increase in Mach number. These apparently conflicting results could be due to differences in such variables as heat transfer, unit Reynolds number, surface

roughness or stream turbulence. To resolve the discrepancies it is necessary to understand more than is presently understood about the combined effects of all of these variables.

In addition to Mach number, a parameter known to be important in determining the extent of laminar flow is the surface roughness. The presence of surface roughness can influence the effect of some other parameter upon transition. For example, the data of reference 6 show that the observed trend of increasing transition Reynolds number with increasing unit Reynolds number in the presence of small granular roughness is reversed if roughness is increased. Again, in references 7 and 8, the favorable effects of cooling (i.e., to increase transition Reynolds number) are shown to be reversed at sufficiently large cooling rates in the presence of surface roughness. It was considered important, therefore, in studying the effect of Mach number on boundary-layer transition, to determine also the simultaneous influence of surface roughness.

The present paper is concerned with an experimental study of these effects in the Mach number range from 2.8 to 7 and for a particular form of two-dimensional distributed roughness. The tests were conducted in the Ames supersonic free flight wind tunnel with fin-stabilized hollow cylinders as test models. The model surfaces were highly cooled with respect to the stagnation temperature. Flow over the external surfaces of the cylinders was considered to approximate closely two-dimensional flow because the laminar boundary-layer thickness was small compared to the cylinder radius and the pitching amplitudes of the models were small.

Results from similar tests using a slender ogive-cylinder as the model have been reported in references 9 and 10. To aid comparison of the present results with those of the previous investigations, a quasi-two-dimensional configuration was tested for which the outer surface of the cylinder was contoured near the leading edge to give approximately the same pressure gradient as that on the ogive-cylinder. Comparative results of the three investigations are discussed herein.

SYMBOLS

C_p pressure coefficient

H roughness height, in. (see fig. 1)

l body nose length, in. (see fig. 1(b))

M Mach number

n number of observations of x_T less than or equal to an arbitrary x

N total number of observations of x_T per model flight

P thread pitch

R Reynolds number, $\frac{Ux}{\nu}$

T_e boundary-layer-edge static temperature, $^{\circ}R$

T_r boundary-layer recovery temperature, $^{\circ}R$

T_t total temperature, $^{\circ}R$

T_w temperature of model surface, $^{\circ}R$

T_∞ free-stream static temperature, $^{\circ}R$

u' velocity perturbation in stream direction, ft/sec

U stream velocity, ft/sec

x axial distance from model leading edge, in.

$\bar{x}_T$ value of x_T for which $\frac{n}{N} = 0.5$ (see fig. 13)

δ thickness of laminar boundary layer, in.

ν kinematic viscosity, ft^2/sec

Subscripts

e boundary-layer-edge value

T transition-point value

∞ free-stream value

MODELS AND TEST PROCEDURE

The tests described in this report were carried out by propelling gun-launched models upstream through the test section of the Ames supersonic free flight wind tunnel. Mach numbers from 2.8 to 4.1 were obtained by firing models through still air ("air-off" testing). Mach numbers from 4.1 to 7 were obtained by firing models through the countercurrent air stream of the wind tunnel ($M = 2$; "air-on" testing). The state of the boundary layer on each model was observed from spark shadowgraphs, in orthogonal planes, taken of the model at successive points along its flight path. A detailed description of the wind-tunnel equipment and the test techniques employed may be found in reference 11.

Model Geometry

The models were designed to permit observation of the quasi-two-dimensional boundary-layer flow over the external surface of sharp-edged hollow cylinders, the axes of which were parallel to the stream direction. They consisted of fin-stabilized tubes 9 inches in length and 3/4 inch in diameter, machined from 7075-T6 aluminum. Two external profiles were tested: a right circular cylinder to provide zero pressure gradient flow; and a contoured nose (open ogival segment) tangent to a cylinder to provide an initial negative pressure gradient. The geometries and dimensions of these models are shown in figure 1. To achieve an adequate pitch-stability margin it was necessary to shift the center of gravity of each model forward by fabricating a portion of the nose from a dense material. Phosphor bronze was used for this purpose. In figure 1 the bronze portion of each model is shown by crosshatching.

The models were launched from a 1-1/2-inch smooth-bore gun. The fin span of the models was made equal to the gun bore so that the models were self-supported and self-alined in the barrel. The sabot used to drive the model was machined from aluminum and was designed to be aerodynamically stable to avoid hitting the tunnel walls. Attention was also given in its design to minimizing separation disturbances to the model. Figure 2 is a photograph showing the two model types and a launching sabot.

The geometry of the slender ogive-cylinder model used for the test reported in references 9 and 10 is shown in figure 3.

For convenience, the models of figures 1(a), 1(b), and 3 are referred to in the present report as the straight tube, contoured tube, and pencil model, respectively.

Surface Roughness and Leading-Edge Profile

Two types of surface roughness were employed: (1) a continuous screw-thread, and (2) a circumferential scratch polish. Most of the data were obtained with the continuous screwthread. This form of roughness has the advantage of a simply defined geometry, the scale of which can be varied over a wide range. It is also possible to reproduce accurately this form of roughness on any number of models.

Screwthread roughness.- The screwthread was applied to the outer surface of the models beginning 0.10 inch behind the leading edge and ending just forward of the fins. The geometric profile of the thread was a single V having a pitch-to-depth ratio of 5. Thread depths between 0.0001 inch and 0.0021 inch were used. The threading detail is shown in figure 1. The initial choice of pitch-to-depth ratio was somewhat

arbitrary, but a fairly large thread angle was dictated by the machining requirements of cleanness of cut and of tool life. In starting the thread the lathe spindle was turned slowly by hand while the tool was fed gradually into the work, one and a half turns being required to reach full thread depth. The surface was then undercut slightly to ensure a full profile with sharp peaks.

All threaded surfaces were examined under the microscope and photographed to provide accurate records of their dimensions. Coarse threads were observed in shadow profile. Fine threads were observed with the aid of an ingenious application by Tolansky (ref. 12) of a principle of optical sectioning developed by Schmalz (ref. 13). This application makes use of the optics of the microscope to cast the shadow of a fine wire obliquely onto the threaded surface. The resulting shadow profile gives a measure of dimensions normal to the surface. Photomicrographs of a typical screw-thread in profile obtained using the wire shadow technique are compared in figure 4.[1]

Example of the smallest and largest threads used are shown in figures 5(a) and 5(b). Some rounding at the peaks and roots of the profiles is evident. Representative measurements of pitch and depth were made on all threaded models. In figure 6 these measurements are shown as the ratio of pitch to depth. The discrepancies observed were due almost entirely to imperfect peaks and roots. In the turning of the finest threads some plastic flow of the metal occurred randomly, causing them to be too deep rather than too shallow.

Threads could not be cut immediately behind the leading edge because of the thinness of the tube wall. To provide a uniformly smooth and known surface, the area between the leading edge and the first thread was given a circumferential scratch polish with grade 2/0 emery paper. The surface profile of this section was first cut to coincide as closely as possible with the extended locus of the thread peaks (see fig. 1) in order to minimize disturbances to the flow. The residual mismatch at the first thread was kept within 0.0003 inch with the unthreaded section high. A representative profile at this station is illustrated in figure 5(c). In this case the peaks of the first few threads have been flattened by the polishing of the forward surface.

Scratch-polish roughness.- The scratch polish was applied to the initial surface of all of the threaded models and to the entire surface of four of the straight-tube models. This surface was produced with fine emery paper using kerosene as a lubricant. Starting with a finish-machined surface, the models were polished with successively finer grades of emery paper until the desired finish was attained. With each change of emery grade the direction of polishing motion was also changed to permit the scratches of the new grade to be distinguished from those of the

[1]The reticle scale, which appears in all of the photomicrographs, cannot be used for direct dimensional comparison in this and subsequent figures because the scale calibration depends upon the power of the microscope objective.

previous grade. Polishing was then continued until examination under the microscope showed that all of the scratches of the previous grade had been removed. The final polish was applied in the circumferential direction.

Examples of the surface finish produced by this technique on 7075-T6 aluminum alloy are shown in the photomicrographs of figure 7. Figures 7(a) and 7(b) show wire-shadow profiles of the 2/0 and 4/0 finishes, respectively. The sensitivity of the wire shadow is not sufficient to resolve the 4/0 profile. Figure 7(c) is an interferogram of the same 4/0 surface. Fringe spacing is 10 microinches. The maximum scratch depths measured on the 2/0 and 4/0 surfaces were approximately 50 microinches and 8 microinches, respectively. These values apply also to the respective surfaces on phosphor bronze.

Leading edge.- The leading edge of each model was carefully worked over with emery paper until a flat forward-facing surface was produced as uniform in width and as thin as practically possible. The corner between the forward-facing surface and the outer surface of the tube was kept square. A uniform leading-edge thickness of 0.0003 inch was set as a goal. Average leading-edge thicknesses of 0.0003 to 0.0004 inch were achieved. Because of the eccentricity between the inner and outer walls of a given model, the finished leading edge varied in thickness by about ±35 percent of the average thickness, with the extreme dimensions diametrically opposed. Figures 8(a) and 8(b) are photomicrographs of segments of the forward face of a representative leading edge at the points of maximum and minimum thickness. Figure 8(c) is a wire shadow profile of the 2/0 outer surface of a straight tube at the leading edge, and indicates that the rounding of the corner was nil within the resolution of the wire-shadow technique.

Test Conditions

Mach number.- The test Mach number was varied between 2.8 and 7. This range was dictated by internal choking in the cylinders at Mach numbers below 2.8 and by incipient structural failure due to launching stresses at Mach numbers above 7.

Reynolds number.- Unit Reynolds number $(U/\nu)_\infty$ was held constant at a nominal value of 3 million per inch by pressurizing the wind-tunnel test section for the air-off (still air) shots and by controlling the reservoir pressure for the air-on (countercurrent air stream) shots. A few models were fired in the supersonic free flight underground range at atmospheric pressure during a period when the wind tunnel was unavailable. For these few shots the free-stream unit Reynolds number was approximately 2.3 million per inch. In addition, a few models were tested at unit Reynolds numbers up to 6 million per inch for the purpose of defining the effect of the smaller variations in unit Reynolds number present in the main body of the results.

Surface temperature.- Each model while in the gun barrel was at ambient temperature. This temperature was assumed to prevail on the model surface during the 15 to 25 millisecond time of flight. The validity of this assumption has been examined in reference 9 and found to be reasonable.[2] For this condition the ratio of model surface temperature to free-stream static temperature was 1.0 for air-off testing and 1.8 for air-on testing for which the Mach number of the air stream was 2.

The relationship of the test temperature ratios to the theoretical conditions for infinite laminar boundary-layer stability is illustrated in figure 9. The theoretical boundary calculated by Van Driest (ref. 14) from the theory of Lees and Lin (refs. 15 and 16) is shown as the dotted curve. The boundary for complete stability with respect to two-dimensional disturbances according to the modified theory of Dunn and Lin (ref. 17) is shown as the solid curve. The ratio $(T_w - T_r)/T_t$ is used as the measure of relative heat transfer in order to show the degree of surface cooling and to emphasize the change in heat flow rate with Mach number for the conditions of the test.

Pressure gradient.- To provide a basis for comparison between results from the contoured tube and from the pencil model, the radius of the contoured tube nose ogive was chosen to give a pressure gradient closely approximating that over the nose of the pencil model. The pressure distribution on the pencil model was obtained from the results of Rossow (ref. 18). For the contoured tube two-dimensional shock-expansion theory was used. The theoretical pressure distributions for these models at Mach numbers of 3 and 6 are presented in figure 10. At Mach number 3 the pressure gradients were closely matched on the model noses but differed immediately behind the nose where on the pencil model an adverse gradient existed. At Mach number 6 the pressure gradients were not so closely matched on the model noses but were nearly the same behind the nose.

Surface roughness parameter.- For the screwthread surface, the vertical peak-to-valley distance, H, was taken as a measure of the roughness scale. For the scratch polish, H was defined as the peak-to-valley distance of the deepest scratches. The roughness measure was made dimensionless by

[2]In reference 9 the temperature rise of the model skin due to aerodynamic heating was calculated for the pencil model. It was concluded that during the short time of the model flight the skin temperature increased by less than 1 percent, except in the immediate neighborhood of the tip where a maximum temperature of 300° R above the average skin temperature was found to be possible. Similar calculations for the hollow-tube models show that leading-edge temperatures approximately 230° R at M = 3.5 and 670° R at M = 7 above average skin temperature were possible. The calculations were conservatively based in two respects: (1) heat flow to the skin was considered constant at the initial rate, and (2) the axial temperature gradient was the limiting value determined by assuming the specific heat of the model material to be zero (i.e., the value necessary to conduct heat out of the tip as fast as it is received). The calculated temperature differences, therefore, represent maximum possible values.

forming the parameter $(H/\delta)\sqrt{R_e}$, first proposed by Seiff, which relates the roughness height to the boundary-layer thickness. For laminar flow on a flat plate this parameter has the property of being independent of distance from the leading edge, and is therefore convenient for specifying the scale of distributed roughness on the straight tube. For configurations such as the contoured tube and pencil model on which pressure gradients occur, the roughness parameter is a function of longitudinal position. In figure 11 values of the roughness parameter on these models are compared, at several Mach numbers, in terms of the corresponding constant value on a flat plate. The parameter shows a wide variation on the nose of each model. However, it is virtually constant behind the nose of the contoured tube, and relatively so on the cylinder of the pencil model. It was deemed desirable to specify the value of the roughness parameter on the body cylinder in order to preserve its independence of longitudinal position and to avoid including implicitly in the parameter possible effects of the nose contour on transition. For all data in which $(H/\delta)\sqrt{R_e}$ was used as an independent variable, transition occured on the body cylinder. It was therefore somewhat arbitrarily decided to evaluate the roughness parameter at the transition point, $\overline{x}_T$. In the computations of $(H/\delta)\sqrt{R_e}$, the boundary-layer thicknesses, δ, were calculated by the method outlined by Cohen and Reshotko in references 19 and 20.

Transition Measurements

Each spark shadowgraph taken of a model in flight provided a record of the instantaneous location of transition at two diametrically opposed points on the model. These points are identified in the representative shadowgraphs of figure 12. Since the distance, x_t, from the leading edge to a local transition point is a function of both time and meridian angle on the model, a statistical method was used to determine a single value of x_t by which to define the mean location of transition for a given model flight. From a total of 7 shadowgraphs per flight a maximum of 14 observations of transition-point location could be made. For an arbitrary value of x the ratio of the number of observations of x_t less than or equal to x, to the total number of observations, can be formed. This ratio, n/N, represents statistically the fraction of the boundary layer which is turbulent at the point x. By plotting n/N as a function of x, a distribution curve is obtained which defines the transition region. Typical distribution curves are illustrated in figure 13. For a given distribution curve the transition region lies between the values of x corresponding to the intercepts of the curve at $n/N = 0$ and $n/N = 1$. These two x positions are often referred to as the beginning of transition and the end of the transition, respectively. The value of x for which half of the observations showed the boundary layer to be turbulent $(n/N = 0.5)$ was taken as the length of the laminar run, $\overline{x}_t$. This was the characteristic length used to determine the transition Reynolds number.

Factors Affecting Precision

Angle of attack.- A small amount of model pitching during flight was inevitable. The maximum pitching amplitudes of the models used for data were generally less than $1\text{-}1/2^{\circ}$. As described in references 9 and 10 the effect of angle of attack on the boundary-layer transition can be determined by plotting the individual values of x_T, for a given model flight, against the angle of attack. For pitching amplitudes greater than some value depending on fineness ratio (about 3° for the hollow-cylinder models), a correlation with angle of attack is found from which extrapolation to zero angle of attack appears to give reliable values of x_T corresponding to zero angle of attack. For smaller pitching amplitudes the data do not correlate with angle of attack and are thus considered to be independent of small amounts of pitching. With respect to the hollow-cylinder models, only data in this latter category were used in the present report.

Leading-edge thickness.- While the leading edges of the tube models were made as thin as possible commensurate with reasonable uniformity of dimension, the large unit Reynolds number of the test resulted in leading-edge-thickness Reynolds numbers of the order of 10^3. According to reference 21, transition Reynolds numbers prevailing for this leading-edge-thickness Reynolds number could be perhaps 10 percent higher than those prevailing for a mathematically sharp leading edge. Reference 22 would indicate a somewhat greater difference. Accordingly, the possibility of the presence of a small increment in R_T due to a finite leading-edge thickness is recognized. Such an increment, however, should be nearly constant in all of the data because of the uniformity of leading-edge thickness among the models and therefore should have at most a secondary effect on the observed trends of R_T with Mach number and surface roughness.

Leading-edge distortion due to heating.- It was necessary to consider the possibility that distortion of the leading edge due to heating might influence the transition measurements in an unknown and variable manner. Calculations based on the thermal properties of the material and the estimated limits of leading-edge temperature showed that if the aluminum leading edge of the straight tube should become bell-mouthed as a result of thermal expansion, it would produce a local re-entrant angle of the cylinder profile of the order of 1°. Similar distortion of the bronze leading edge of the contoured tube would be approximately 50 percent greater. Double bow waves were observed in the shadowgraphs of the straight tube. These might be inferred as evidence that temperature distortion of the leading edge was indeed affecting the boundary-layer flow. However, it was also observed on one or two occasions when the leading-edge profile of the straight tube was not square but rounded (under the same test conditions) that the double bow wave did not appear. It is believed therefore that the double bow wave was due to flow separation at the 90° leading-edge corner and subsequent reattachment on the cylinder. Re-entrant flow disturbance due to leading-edge distortion probably would be less than that due to reattachment. No

double bow waves were observed with the contoured tube, probably because the relatively high static pressure at the leading edge prevented flow separation. The effect of leading-edge distortion in this case might be through a slight alteration of the local pressure distribution.

In searching for direct evidence of a leading-edge distortion effect it was anticipated that because of the transient nature of the heating process and consequent progressive distortion of the leading edge the local flow pattern, or the distance to transition, might show a progressive variation with distance flown. However, variations of this sort were not detected. It was concluded that any effects of leading-edge distortion which might be present were both small and, for a given Mach number, constant.

Repeatability of the transition measurements.- The general repeatability of the data is dependent both upon the precision with which the measurements are made and upon the duplication of all aerodynamic and geometric conditions of the test for successive model flights. In these tests the precision of a given data point depended principally on the errors of measurement of x_T. Errors of measurement of the other physical quantities from which Mach number and Reynolds number were determined were of lower orders of magnitude. The value of the characteristic transition distance, $\overline{x}_T$, as determined by the method previously described, was found to be relatively insensitive to the normal uncertainties in the choice of local transition locations from the shadowgraphs. Repetitive determinations of $\overline{x}_T$ usually agreed within approximately 1/8 inch. The corresponding values of R_T therefore are considered to be accurate to within $\pm 1/2$ million.

An indication of the precision with which specified test conditions can be met is given by the repeatability of data from successive models flown under the same set of test conditions. Only a very limited number of such data were obtained with the hollow-cylinder models and these were all for the straight-tube configuration. The available comparisons indicate a repeatability of R_T within ± 1 million for this configuration. Similar comparisons for the pencil model indicate a repeatability of R_T for this model within $\pm 1/2$ million. For the contoured tube it is believed that because the potential leading-edge effects appear to be fewer on this model than on the straight tube, the repeatability of the data from this configuration should be correspondingly more precise. It is believed to approximate that for the pencil model.

EXPERIMENTAL RESULTS

Gross Trends

In order to show graphically the ranges of Mach number and Reynolds number in which the data fall, the transition data are plotted against boundary-layer-edge Mach number in figure 14. The length Reynolds number of the point at which turbulence was first observed is designated by the open symbol. The length Reynolds number of the point beyond which no laminar flow was observed is designated by the filled symbol. For a given model flight each such pair of symbols marks the beginning and the end of the transition region. This figure indicates an over-all trend of increasing transition Reynolds number with increasing Mach number. The increase in transition Reynolds number between Mach number 3 and Mach number 7 is approximately threefold. Within this group of data the average length of the transition region is roughly 7 million Reynolds number, and does not appear to be a function of Mach number.

In this figure, surface roughness is a variable, the variation being more or less random throughout the Mach number range. The transition range for the roughest model (coarse screwthread) is labeled, and gives a preliminary indication of the detrimental effect of large roughness.

Lines of minimum critical Reynolds number according to Van Driest (ref. 14) are shown in figure 14 for the two values of wall to free-stream temperature ratio which prevailed in the present test. The minimum critical Reynolds number is defined in the stability theory of Lees and Lin (refs. 14, 15, and 16) as the Reynolds number below which small disturbances in the laminar boundary layer are damped, and above which they are amplified. Transition is shown to have occurred, on models of the present test, at Reynolds numbers below the minimum critical, and the trend of transition Reynolds number with Mach number appears to be continuous through the minimum critical Reynolds number.

Consideration has been given to the possible effects on the test results of the simultaneous changes in wall to local static temperature ratio and stream turbulence at $M_e = 4.1$. It would be expected, because of the higher cooling rate, that transition would occur at a higher Reynolds number below $M_e = 4.1$ than above it. At the same time the absence of stream turbulence below $M_e = 4.1$ should tend to induce a higher transition Reynolds number below $M_e = 4.1$ than above. Therefore the potentially detrimental effects on transition of the discontinuous changes in temperature ratio and turbulence level[3] are additive and, if

[3] The turbulence level of the wind-tunnel air stream is not known quantitatively. However, the effective turbulence experienced by the moving model is, because of its own velocity, only about a third of that which would be experienced by a static model in the same air stream.

significant, should be observable in the data. In figure 14 there is no sensible discontinuity in the trend of the data at $M_e = 4.1$. Likewise in subsequent presentations there are no observable discontinuities at $M_e = 4.1$. It is concluded that such effects are not significant in the present results. In reference 10 similar reasoning was used to reach the same conclusion with respect to data for the pencil model.

Effect of Mach Number

To see more clearly the separate effect of Mach number on boundary-layer transition the data are plotted separately for each configuration and for constant roughness height, H. In figure 15 the variations of transition Reynolds number with Mach number on the contoured tube, the pencil model, and the straight tube are compared. The data of figure 15(b) are reproduced from reference 10. Curves of constant surface roughness (nominal thread height, H) are faired through the data. It is clear that for a variety of test conditions, transition Reynolds number increases with increasing Mach number. It is further apparent that the sensitivity of transition Reynolds number to Mach number variation is dependent on the ranges of Mach number and roughness prevailing. Point by point comparisons between the data of figure 15(a), (b), and (c) indicate that transition Reynolds numbers differ on the different configurations for given conditions of Mach number and roughness height. In general the highest values of R_T occur on the contoured tube, while the comparison between the pencil model and straight tube appears inconclusive. However, a basis for a more critical comparison of these data is established in the discussion section and the effects of configuration are subsequently considered in more detail.

Effect of Surface Roughness

To show the effect of roughness on transition, the same data are plotted in figure 16 with surface roughness height, H, as the independent variable. Curves of constant Mach number are faired through the data. The manner of fairing of figures 15 and 16 was influenced by the fact that since each is a cross plot of the other, the fairings must be mutually consistent. Figures 16(a) and (b) show that gross increases in roughness height produce substantial reductions in transition Reynolds number. As before, it may be observed that the sensitivity of transition Reynolds number to roughness variation is dependent on the ranges of roughness and Mach number prevailing.

An interesting phenomenon revealed in these figures is that for this type of roughness, on the models having a favorable pressure gradient over the nose at least, the maximum length of laminar run does not occur on the smoothest surface, but on a surface having appreciable roughness. The

optimum roughness is dependent on Mach number and is seen to be not far below the roughness which will cause the laminar run to be a minimum. The increase in R_T above the value for a smooth surface appears to be approximately 10 to 15 percent of the smooth surface value. The relatively large increase in R_T with increasing roughness height indicated by the data in figure 16(a) for nominal Mach numbers of 3.0 and 3.7 are believed to be exaggerated as the result of an anomalous roughness characteristic affecting the two points having nominal roughness heights of 120 μin. The values of R_T represented by these points are believed to be low because the screwthread roughness on the corresponding models was imperfectly formed. In cutting the threads on these two models the lathe tool threw up small ridges of nonuniform height along the thread peaks. These ridges introduced a three-dimensional quality to the roughness on these models. It is known that a three-dimensional roughness of a given height has a greater effectiveness in causing transition than has a two-dimensional roughness of the same height. For example, Carros observed over a range of Mach numbers (see fig. 15(b)) that a sandblasted surface having a maximum roughness height of 1000 μin. caused earlier transition than did a screwthread of 1500 μin. height. The roughness characteristic just described was confined to the two models in question and therefore does not explain the appearance of an optimum roughness at the higher Mach numbers. This phenomenon is examined in more detail in the discussion section.

Effect of Unit Reynolds Number

Published results of earlier transition experiments (e.g., refs. 23 through 27) show that, for small roughness, transition Reynolds number increases as unit Reynolds number increases. For this reason it was considered important to hold unit Reynolds number constant in the present experiment and this was done, within experimental accuracy, for most of the data. Two situations developed, however, which made it desirable to assess, at least roughly, the effect of unit Reynolds number variation on R_T for values of U/ν of the order of 3 million per inch. The first was the fact that unit Reynolds number for the underground range shots could not be controlled independently of Mach number. The second was the desire to make comparisons between the present results and those obtained with the pencil model at lower unit Reynolds numbers.

To provide a basis for assessment of the effect of unit Reynolds number variation on the test results a very few data points were obtained with the straight tube and pencil model to determine the variation of transition Reynolds number with unit Reynolds number for constant Mach number and subcritical roughness height (i.e., roughness height less than that required to influence transition). In figure 17 these data are compared with results of the earlier investigations. The trend of R_T with $(U/\nu)_\infty$ observed in the present range of unit Reynolds numbers appears to be the same as that observed previously on similar configurations at lower unit

Reynolds numbers. It is to be emphasized that comparisons should be made between slopes of the individual curves rather than between specific values of R_T. On the log-log presentation of figure 17 most of the curves can be approximated by the relation

$$\log_{10} R_T = C_1 + C_2 \log_{10} \left(\frac{U}{\nu}\right)_\infty$$

where C_1 and C_2 are constants for a given curve. The value of C_1 is dependent on many variables including Mach number, surface roughness, and surface cooling. The slope, C_2, appears to be considerably less sensitive to these variables (at least for subcritical roughness). It is believed that figure 17 provides a satisfactory basis for accounting for the effects of relatively small differences in $(u/\nu)_\infty$ in comparisons of transition data obtained at different unit Reynolds numbers, if roughness is subcritical. The average value of C_2 for all the curves of figure 17 is 0.40. This value was used to adjust data for three of the underground range shots.

DISCUSSION

Mach Number and Roughness Effects on the Contoured Tube

Cross plots of the data.- To define precisely each of the highly nonlinear curves of figures 15 and 16 would require many more data points than were obtained in the present investigation. Therefore, in order to gain a more complete understanding of the behavior of boundary-layer transition under varying Mach number and roughness conditions, advantage was taken of the fact that figures 15 and 16 are mutual cross plots. Attention was focused on the data from the contoured tube since these were the most complete and were obtained under the most precisely controlled conditions. Two cross-plot families of curves were constructed about the data of figures 15(a) and 16(a). The fairings of these curve families were iterated between the figures first assuming the data to have absolute precision and then allowing the curves to miss individual data points by the amount necessary to obtain quantitative consistency of the curve families. In making these plots, surface roughness was made dimensionless through the use of the parameter $(H/\delta)\sqrt{R_e}$ discussed under test conditions. The quantitatively consistent cross plots resulting from this procedure are shown in figures 18 and 19. Unit Reynolds number is constant and equal to 3.1 million per inch.[4] These figures are discussed separately in the following paragraphs.

[4]Transition Reynolds numbers of three data points from the underground range, for which surface roughness was below critical values, were adjusted on the basis of figure 17 to correspond to this unit Reynolds number. Single-flagged symbols identify these points.

Three other data points from the range (double-flagged symbols), for which roughness was supercritical, were not adjusted because no suitable basis was available. Data from reference 6 indicate qualitatively that such adjustments should be smaller than - or even of opposite sign to - those for subcritical roughness.

Effect of Mach number.- In figure 18, transition Reynolds number is plotted against local Mach number for constant values of the roughness parameter. According to this figure, as Mach number increases, for a given surface roughness, R_T increases slowly along the curve A-A until a critical Mach number is reached; R_T then increases rapidly until a second critical Mach number is reached at the envelope curve B-B; R_T then increases more slowly with the rate of increase approaching a nearly constant value along curve C-C with further increase in Mach number. On a sufficiently rough surface, then, R_T increases with M_e at a rate indicated by the curve A-A, and on a sufficiently smooth surface R_T increases with M_e at a rate indicated by the curve C-C. The reason for this difference in rate is not clearly understood. It has been pointed out in reference 10 that for a constant wall to local static temperature ratio the relative cooling effect of the wall increases with Mach number. This fact is evident also from an examination of figure 9. For such a condition it would be expected on the basis of stability theory that the boundary layer would remain laminar to higher Reynolds numbers as Mach number increases. This is in agreement with the observed variation. The effect of heat-transfer variation (surface cooling) is implicit in the Mach number variation, however, and therefore it cannot be ascertained just what fraction of the observed increase in R_T is due to increasing heat transfer. Results from references 4, 5, 7, and 25 are compared with the present results for the contoured tube in figure 20, where the curve C-C of figure 18 is reproduced. The effect of roughness is believed to be insignificant in these data, at least at the higher Mach numbers, so that the data are most nearly comparable to curve C-C. Other test conditions (e.g., unit Reynolds number, initial pressure gradient) differ significantly, however, and the curves cannot be quantitatively compared. They should be compared only as to trend. The variation observed in the data of reference 7 for the cooled cone (T_w/T_e = const) is similar to that observed in the present test. On the other hand results from the insulated cone and flat plates show a trend of decreasing R_T with increasing Mach number below a Mach number of about 3.8 but a reversal of the trend above this Mach number. It appears therefore that while the differences in trend below $M_e = 3.8$ may be due to the effect of heat transfer, other effects are also present which in addition to surface cooling tend to delay transition as Mach number increases. These effects are as yet unidentified.

Effect of roughness.- In figure 19, transition Reynolds number is plotted against the roughness parameter, $(H/\delta)\sqrt{R_e}$, for constant values of Mach number. As the roughness parameter increases, for a given Mach number, R_T increases gradually to a maximum at some critical value of the roughness parameter; R_T then decreases rapidly until a second critical value of the roughness parameter is reached, after which R_T tends to remain constant (at least at $M_e = 3$) with further increase in $(H/\delta)\sqrt{R_e}$. Figure 19 indicates the existence of two families of critical combinations of Mach number and surface roughness. One family represents conditions for maximum transition Reynolds number. The other family represents the minimum roughness which gives the minimum value of transition Reynolds number. The loci of these combinations are indicated in the figure by the dashed lines.

These lines separate the plot into three distinct regions of transition Reynolds number variation: Region I in which R_T is relatively low and is only moderately sensitive to changes in Mach number; region II in which R_T varies rapidly with either Mach number or surface roughness; region III in which R_T is relatively high and has intermediate sensitivity to changes in Mach number and roughness.

Optimum roughness phenomenon.- The appearance of an optimum roughness height corresponding to the maximum laminar run at a given Mach number was unexpected. The mechanism which operates to produce this phenomenon is not yet understood. It is tentatively thought to be associated with the shape of the roughness. According to figures 18 and 19 this effect becomes increasingly significant as Mach number increases. The only other evidence yet found of the existence of such a phenomenon comes from a recent investigation of roughness effects in low speed flow. In reference 28 the transition Reynolds numbers on a two-dimensional surface with and without a single transverse wire were compared at $M_e < 0.17$. In two instances, where the wire was relatively close to the leading edge, the data show that an optimum ratio of roughness height to laminar-boundary-layer momentum thickness occurred in a way very similar to that observed in the present investigation. There was no significant increase in transition Reynolds number, however.

A possible mechanism whereby the transverse screwthread type of roughness could either produce or damp disturbances in the boundary layer is suggested by the results of some experiments with single transverse rectangular cutouts reported in references 29 and 30. In these experiments acoustic radiation (periodic pressure waves) was observed to emanate from the cutouts for certain combinations of Mach number and cutout dimensions. It was shown that in the Mach number range 0.4 to 1.5 the frequency of the radiation increased with increasing Mach number if the gap width was held constant and that the gap width necessary to maintain a constant frequency increases with increasing Mach number. Vortex motion was observed within the cutout, and under certain conditions vortices appeared to be shed periodically from the cutout. In the Ames supersonic free flight wind tunnel, acoustic radiation occasionally has been observed to emanate from screwthreads and transverse V-shaped grooves on models in supersonic free flight. An example of this radiation is illustrated in figure 21, which shows a short thin-walled hollow cylinder flying at a Mach number of 1.23. The radiation originates at a group of five circumferential V-grooves, each 0.003-inch deep, located a short distance behind the leading edge. It may be inferred that the flow pattern in each groove of a screwthread is similar to the flow in the rectangular cutout. A captive vortex in a thread groove could act as an energy reservoir which under the proper flow conditions could absorb and redistribute energy perturbations in the boundary layer and thus be a damping device. The vortex, whose size is determined by the size of the groove, must have the proper characteristics to resonate with the boundary-layer perturbations. If the groove were much too small, the vortex would not form. If the groove were much too large, the vortex might become unstable and shed into the boundary layer

causing a large disturbance (acoustic radiation). Since the energy which drives the vortex comes from the main stream, it might be expected that the combination of Mach number and groove size required to produce resonance damping would vary qualitatively in the same way as that required to produce acoustic radiation. Figure 19 indicates that as Mach number increases the groove size required to obtain the maximum laminar run also increases, so that this combination does in fact vary in a manner consistent with the above expectation. In the case of the transverse wire of reference 28 a vortex flow in the separated regions immediately forward and aft of the wire could provide resonance damping of boundary-layer oscillations. On the other hand, the shape of the curve for the sandblasted surface in figure 15(b) makes it appear that an optimum roughness height may occur for this type of roughness. If such is the case then the above hypothesis must be modified.

In any event the transverse groove or screwthread, under the present test conditions, has the demonstrated ability to prolong laminar flow to a higher Reynolds number than can an extremely smooth surface. At the higher Mach numbers the optimum roughness resulted in transition Reynolds numbers 15 percent higher than would be obtained with much smaller roughness. The optimum roughness height at these Mach numbers was 8 to 10 percent of the laminar boundary-layer thickness at transition. The corresponding full-scale roughness height could be of the order of 0.1 inch. This result suggests the possibility of submerging miscellaneous surface imperfections which are potential sources of turbulence (such as joints and rivet heads) by applying a uniform transverse groove finish to the surface of an assembled wing or body. In addition, based on the theoretical results of Chapman (ref. 31) there appears the possibility of reducing total heat transfer and total skin friction by using the continuous screwthread to produce controlled regions of separated flow. Such a possibility would seem to warrant further investigation.

Critical combinations of Mach number and roughness parameter.- Curves of the critical combinations of Mach number and roughness parameter observed in figure 19 are plotted in figure 22. The three regions into which the curves divide this plot correspond to those of figure 19; so that under the present test conditions, for combinations of Mach number and roughness parameter which fall into Region I, the presence of roughness will result in minimum values of R_T while, for combinations which fall into Region III, roughness will have no adverse effect on R_T. Figure 22 shows rather clearly that as Mach number increases the laminar boundary layer is able to negotiate increasingly rough surfaces before transition is influenced adversely by the roughness. It is also evident that the incremental increase in roughness necessary to reduce R_T to a minimum (Region II) becomes greater as Mach number increases. In other words the adverse effect of roughness on transition is not as abrupt at high Mach numbers as it is at low Mach numbers.

Comparison of Results From the Three Models

Although the curves of figures 15 and 16 for the pencil model and straight tube do not present as complete nor as consistent a pattern of variation as do the curves for the contoured tube, it is apparent that the qualitative effects of Mach number and surface roughness on transition Reynolds number are similar on all three models, and it is possible through comparison with the complete patterns of figures 18 and 19 to identify these data with respect to the trend regions defined in figures 19 and 22. Such indications as there are of the critical values of roughness height and Mach number for the pencil model and straight tube, when compared with the corresponding values for the contoured tube, suggest that these values do not vary greatly among the three configurations considered. However, rather consistent differences in transition Reynolds number are seen to exist between the curves for one configuration and the corresponding curves for another. For example, looking at figures 15 and 16, parts (a) and (b), it is apparent that an upward translation of approximately 3 million Reynolds number of the curves for the pencil model would put them into closer agreement with those for the contoured tube. With respect to the straight tube, no models having large roughness were tested. Figure 16(c) shows that the data for this model were confined to roughness values generally less than those which figure 15(a) shows to be optimum for the contoured tube. This suggests that the straight-tube data for the higher Mach numbers at least, should fall within Region III as defined in figures 19 and 22. It follows that the straight-tube data in figure 15(c) should be comparable to the curve C-C of figure 18. A comparison shows the agreement to be reasonably good. As was observed with the pencil model, however, the agreement would be improved if the data for the straight tube were translated upward by approximately 3 million Reynolds number. In the case of the pencil model, approximately a third of this difference can be attributed to the difference in $(U/\nu)_\infty$. Otherwise these roughly constant differences in R_T between the curves of one configuration and those of another reflect the influence of configuration change on the environment of the laminar boundary layer.

Among the three configurations there are three important differences in the boundary-layer environment:

1. Pressure gradient
2. Relative surface roughness on the nose
3. Local flow separation at the leading edge

The first two of these are apparent from figures 10 and 11.

Considering pressure gradient alone, it would be expected that transition would be delayed on the contoured tube and pencil model to higher Reynolds numbers than on the straight tube. On the other hand, the roughness over the noses of these two models, in terms of boundary-layer thickness, is considerably greater than on the straight tube. This condition would be expected to have a detrimental effect which would oppose the favorable effect of pressure gradient.

The adverse pressure gradient aft of the nose of the pencil model is small compared to the favorable gradient over the nose. At Mach number 6 it almost disappears. The major difference, therefore, between the flow conditions over the pencil model and the contoured tube is in the relative surface roughness over the nose. The relative roughness over the nose of the pencil model is in the neighborhood of 50 to 75 percent greater than that over the nose of the contoured tube. This difference could be responsible for the lower transition Reynolds numbers on the pencil model.

The third difference in boundary-layer environment is that of local flow separation at the leading edge. This local separation at the leading edge of the straight tube is illustrated in figures 12(d) and (e) where the separation bubble is betrayed by the double bow wave. The contoured tube (figs. 12(a), (b), and (c)) and the pencil model do not show evidence of leading-edge separation. In spite of the sharpness of the leading edges and the large value of unit Reynolds number, local separation occurred on all models of the straight tube. While the effect of this local separation on the transition Reynolds number is undoubtedly adverse, its magnitude is not known. It is therefore not possible to use the straight-tube results as a standard by which to judge the relative importance of pressure gradient and roughness on the other two models. It is believed, however, that this effect could have reduced significantly the laminar flow on the straight tube. It is believed to have been responsible for the greater scatter in R_T observed for this model.

CONCLUSIONS

The effects of Mach number and a screwthread form of distributed two-dimensional surface roughness on boundary-layer transition were investigated on hollow-cylinder models in free flight at Mach numbers between 2.8 and 7. The model surfaces were cold relative to stagnation temperatures and the rate of boundary-layer cooling was a function of Mach number. The observed effects were compared with results previously obtained on a slender ogive-cylinder. The results of these tests are summarized in the following conclusions:

1. Transition Reynolds number increased with increasing Mach number for all magnitudes of roughness tested.

2. The minimum size of roughness which will influence transition increases with increasing Mach number. The effect of a given roughness size was found to depend strongly on the Mach number.

3. For a given Mach number, an optimum value of roughness height was found which gave a maximum laminar run 10 to 15 percent greater than was obtained with very small roughness. This optimum roughness height at the higher Mach numbers was 8 to 10 percent of the laminar boundary-layer thickness at transition.

Ames Research Center
National Aeronautics and Space Administration
Moffett Field, Calif., Oct. 22, 1958

REFERENCES

1. Lee, Roland E.: Measurements of Pressure Distribution and Boundary-Layer Transition on a Hollow-Cylinder Model. NAVORD Rep. 2823, April 28, 1953.

2. Czarnecki, K. R., and Sinclair, Archibald R.: Factors Affecting Transition at Supersonic Speeds. NACA RM L53I18a, 1953.

3. Gazley, Carl, Jr.: Boundary-Layer Stability and Transition in Subsonic and Supersonic Flow. Jour. Aero. Sci., vol. 20, no. 1, Jan. 1953, pp. 19-28.

4. Laufer, John, and Marte, Jack E.: Results and a Critical Discussion of Transition-Reynolds-Number Measurements on Insulated Cones and Flat Plates in Supersonic Wind Tunnels. CIT, JPL Rep. 20-96, Nov. 30, 1955.

5. Korkegi, Robert H.: Transition Studies and Skin-Friction Measurements on an Insulated Flat Plate at a Mach Number of 5.8. Jour. Aero. Sci., vol. 23, no. 2, Feb. 1956, pp. 97-107.

6. Luther, Marvin: Fixing Boundary-Layer Transition on Supersonic-Wind-Tunnel Models. CIT, JPL Progress Rep. 20-256, Aug. 12, 1955.

7. Van Driest, E. R., and Boison, J. Christopher: Experiments on Boundary-Layer Transition at Supersonic Speeds. Jour. Aero. Sci., vol. 24, no. 12, Dec. 1957, pp. 885-899.

8. Jack, John R., Wisniewski, Richard J., and Diaconis, N. S.: Effects of Extreme Surface Cooling on Boundary-Layer Transition. NACA TN 4094, 1957.

9. Jedlicka, James R., Wilkins, Max E., and Seiff, Alvin: Experimental Determination of Boundary-Layer Transition on a Body of Revolution at $M = 3.5$. NACA TN 3342, 1954. (Supersedes NACA RM A53L18)

10. Carros, Robert J.: Effect of Mach Number on Boundary Layer Transition in the Presence of Pressure Rise and Surface Roughness on an Ogive-Cylinder Body With Cold Wall Conditions. NACA RM A56B15, 1956.

11. Seiff, Alvin: A Free-Flight Wind Tunnel for Aerodynamic Testing at Hypersonic Speeds. NACA Rep. 1222, 1955. (Supersedes NACA RM A52A24)

12. Tolansky, Samuel: A Topographic Microscope. Scientific American, vol. 191, no. 2, Aug. 1954, pp. 54-59.

13. Schmalz, G.: Technische Oberflächenkunde, Julius Springer Verlag, Berlin, 1936.

14. Van Driest, E. R.: Calculation of the Stability of the Laminar Boundary Layer in a Compressible Fluid on a Flat Plate with Heat Transfer. Jour. Aero. Sci., vol. 19, no. 12, Dec. 1952, pp. 801-812, 828. (Also available as North American Aviation Rep. AL-1334, Feb. 1952)

15. Lees, Lester, and Lin, Chia-Chiao: Investigation of the Stability of the Laminar Boundary Layer in a Compressible Fluid. NACA TN 1115, 1946.

16. Lees, Lester: The Stability of the Laminar Boundary Layer in a Compressible Fluid. NACA Rep. 876, 1947. (Supersedes NACA TN 1360)

17. Dunn, D. W., and Lin, Chia-Chiao: On the Stability of the Laminar Boundary Layer in a Compressible Fluid. Jour. Aero. Sci., vol. 22, no. 7, July 1955, pp. 455-477.

18. Rossow, Vernon J.: Applicability of the Hypersonic Similarity Rule to Pressure Distributions Which Include the Effects of Rotation for Bodies of Revolution at Zero Angle of Attack. NACA TN 2399, 1951.

19. Cohen, Clarence B., and Reshotko, Eli: Similar Solutions for the Compressible Laminar Boundary Layer With Heat Transfer and Pressure Gradient. NACA Rep. 1293, 1956. (Supersedes NACA TN 3325)

20. Cohen, Clarence B., and Reshotko, Eli: The Compressible Laminar Boundary Layer With Heat Transfer and Arbitrary Pressure Gradient. NACA Rep. 1294, 1956. (Supersedes NACA TN 3326, 1955)

21. Brinich, Paul F., and Sands, Norman: Effect of Bluntness on Transition for a Cone and a Hollow Cylinder at Mach 3.1. NACA TN 3979, 1957.

22. Bertram, Mitchel H.: Exploratory Investigation of Boundary-Layer Transition on a Hollow Cylinder at a Mach Number of 6.9. NACA Rep. 1313, 1957. (Supersedes NACA TN 3546)

23. Potter, J. L.: New Experimental Investigations of Friction Drag and Boundary Layer Transition on Bodies of Revolution at Supersonic Speeds. NAVORD Rep. 2371, April 1952.

24. Evvard, J. C., Tucker, M., and Burgess, W. C., Jr.: Statistical Study of Transition-Point Fluctuations in Supersonic Flow. NACA TN 3100, 1954.

25. Coles, Donald: Measurements of Turbulent Friction on a Smooth Flat Plate in Supersonic Flow. Jour. Aero. Sci., vol. 21, no. 7, July 1954, pp. 433-448.

26. Brinich, Paul F.: Boundary-Layer Transition at Mach 3.12 With and Without Single Roughness Elements. NACA TN 3267, 1954.

27. Brinich, Paul F.: A Study of Boundary-Layer Transition and Surface Temperature Distributions at Mach 3.12. NACA TN 3509, 1955.

28. Smith, A. M. O., and Clutter, D. W.: The Smallest Height of Roughness Capable of Affecting Boundary-Layer Transition in Low-Speed Flow. Douglas Aircraft Co. Rep. no. ES 26803, Aug. 31, 1957.

29. Krishnamurty, K.: Acoustic Radiation From Two-Dimensional Rectangular Cutouts in Aerodynamic Surfaces. NACA TN 3487, 1955.

30. Roshko, Anatol: Some Measurements of Flow in a Rectangular Cutout. NACA TN 3488, 1955.

31. Chapman, Dean R.: A Theoretical Analysis of Heat Transfer in Regions of Separated Flow. NACA TN 3792, 1956.

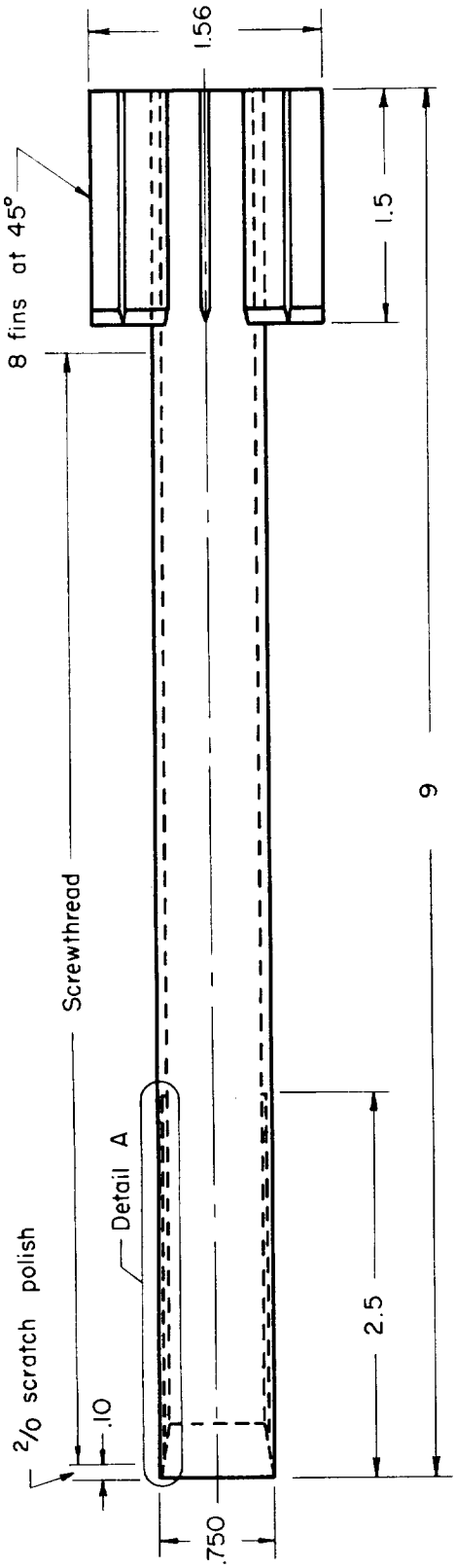

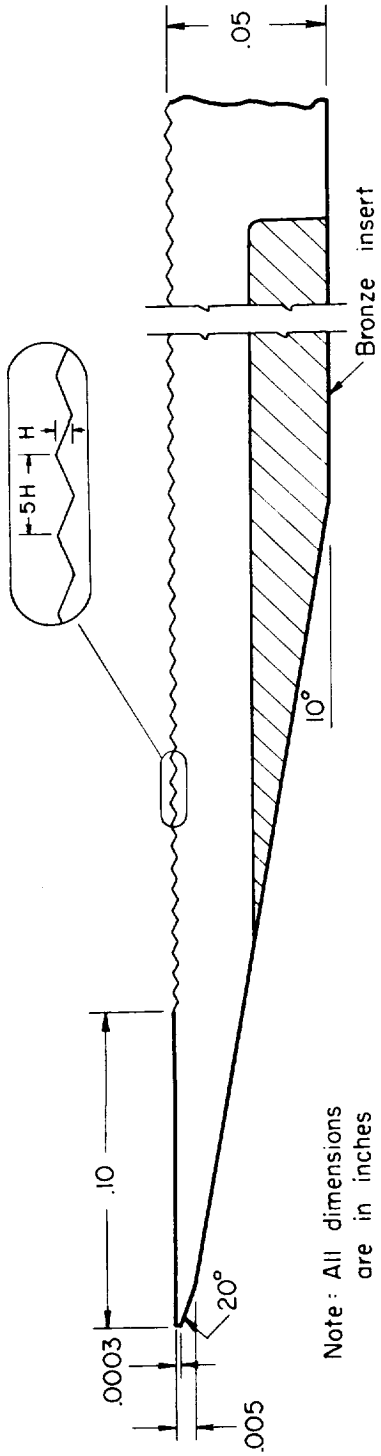

(a) Straight tube.

Figure 1.- Details of test models.

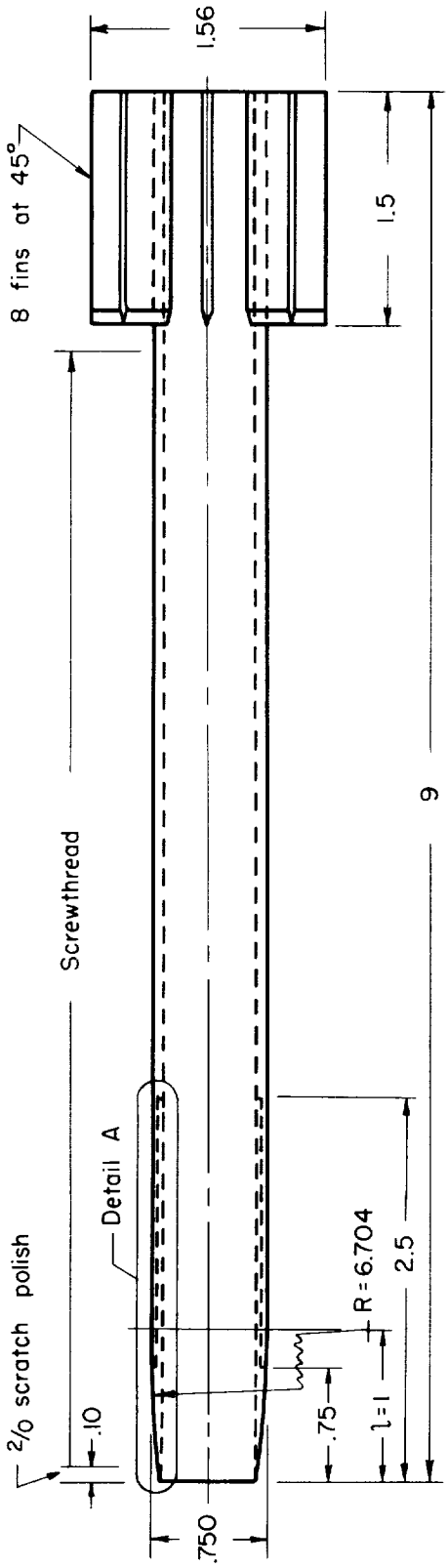

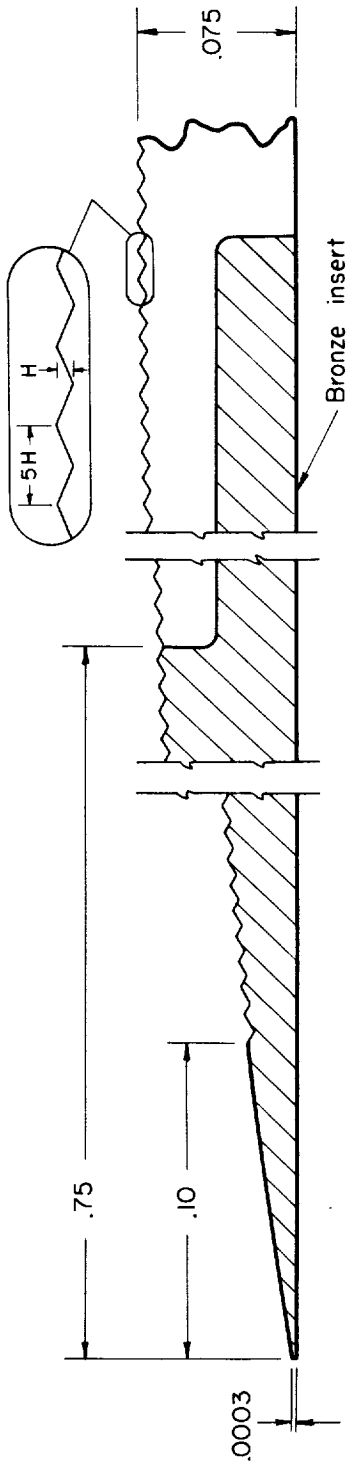

(b) Contoured tube.

Figure 1.- Concluded.

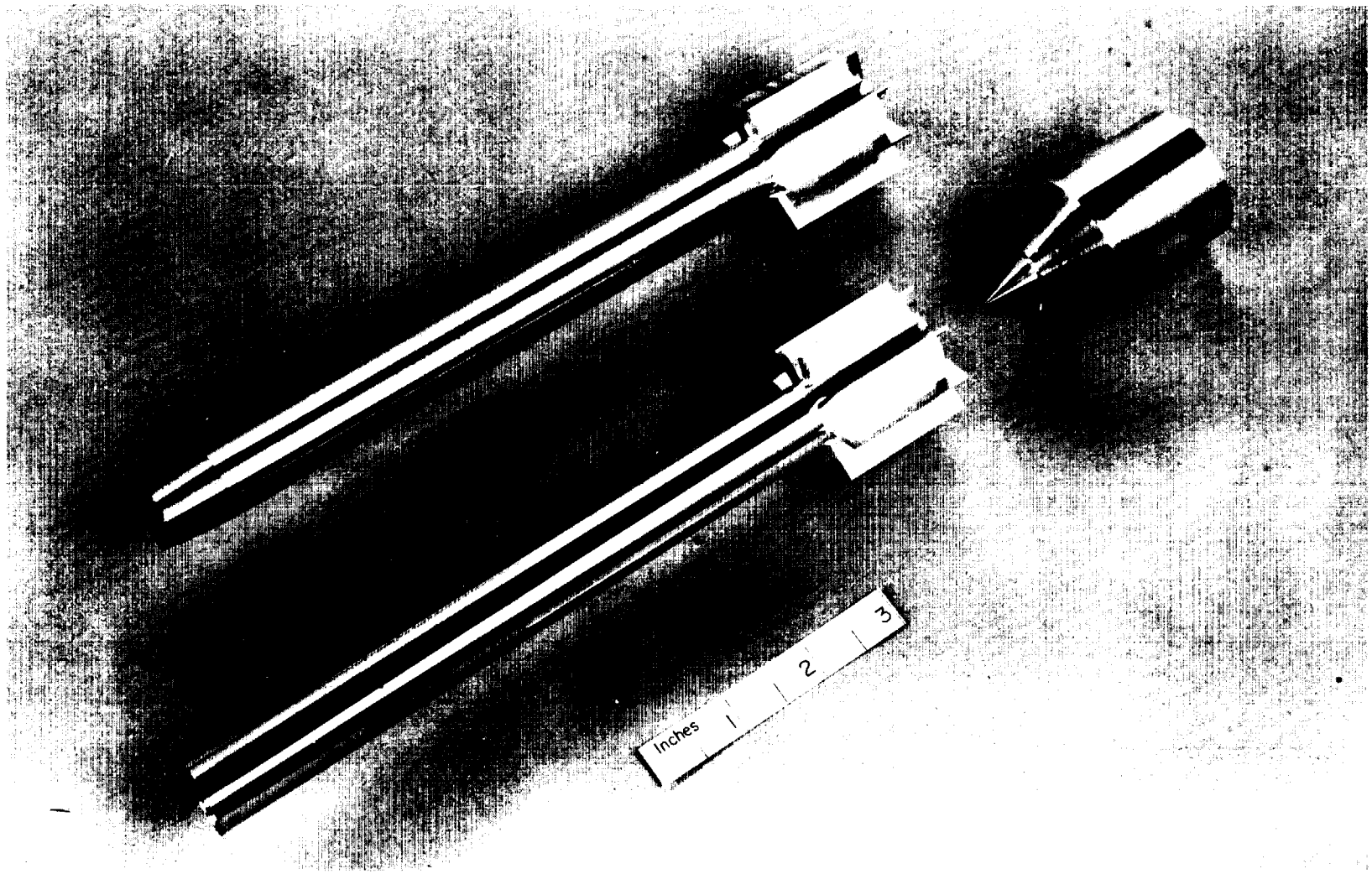

A-21715

Figure 2.- Photograph of the two model configurations and a sabot.

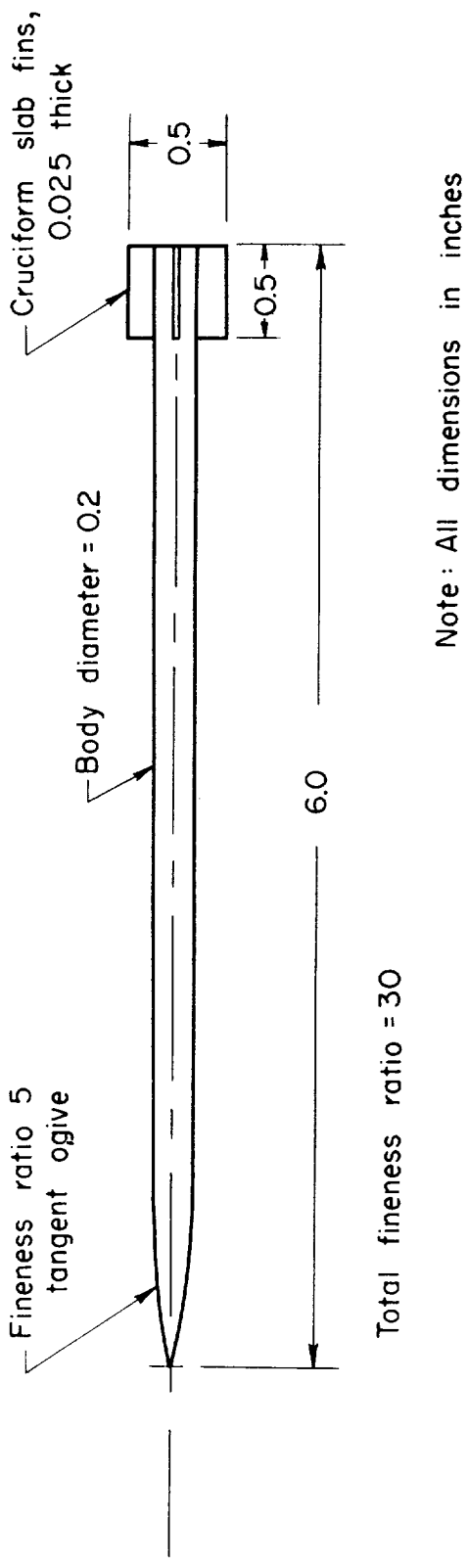

Figure 3.- Ogive-cylinder (pencil model) of references 9 and 10.

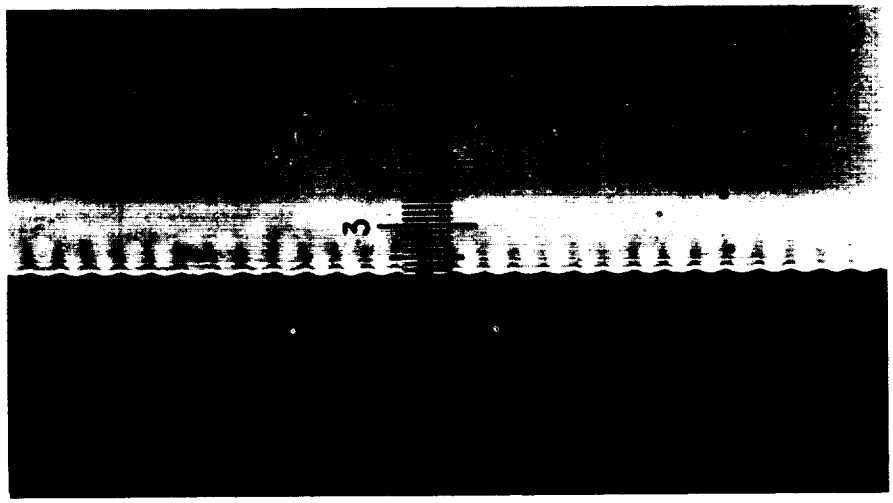

(a) Shadow profile, 100X.

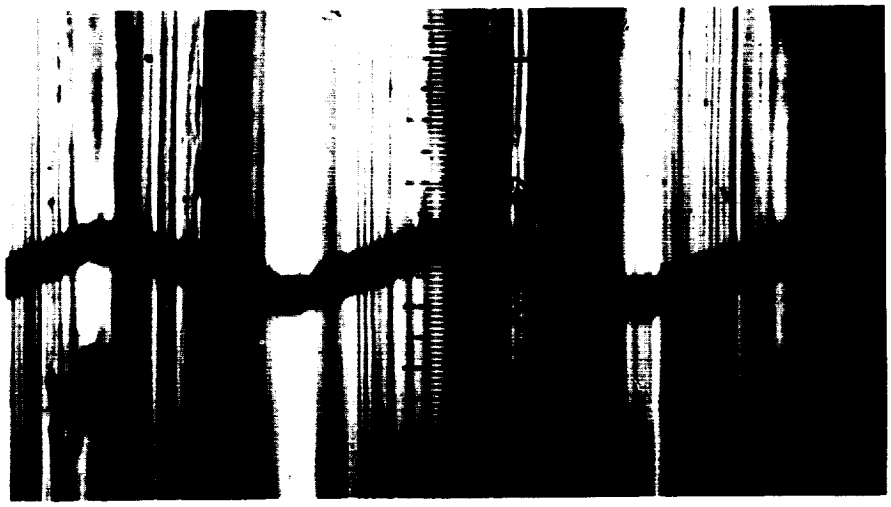

(b) Wire shadow, 1000X.

Figure 4.- Photomicrographs of a typical screwthread; depth = 0.0003 inch; pitch = 0.0015 inch.

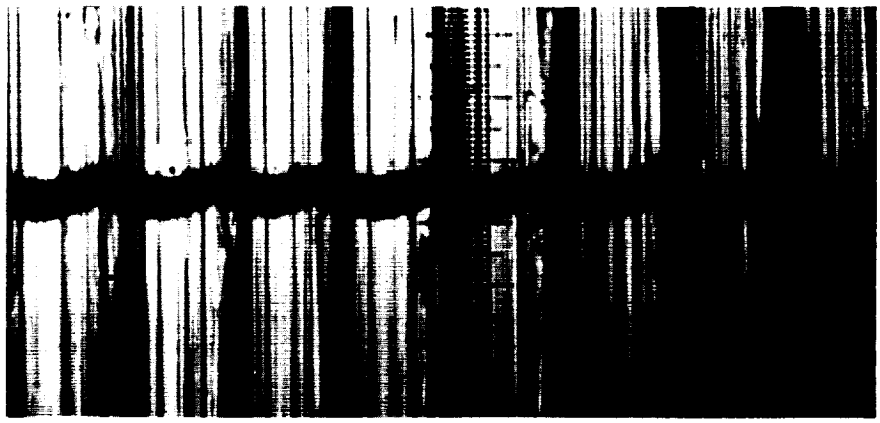

(a) Fine screwthread, 0.00008 inch deep; wire shadow; 1000X.

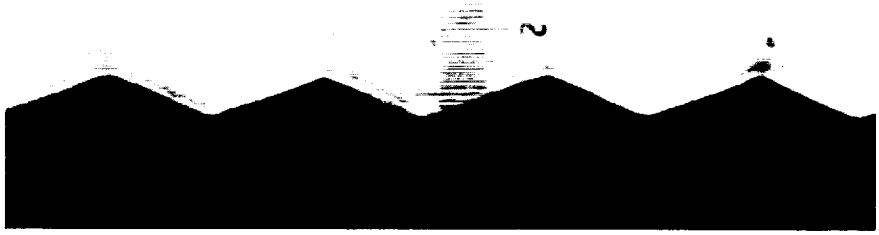

(b) Coarse screwthread, 0.0021 inch deep; profile; 100X.

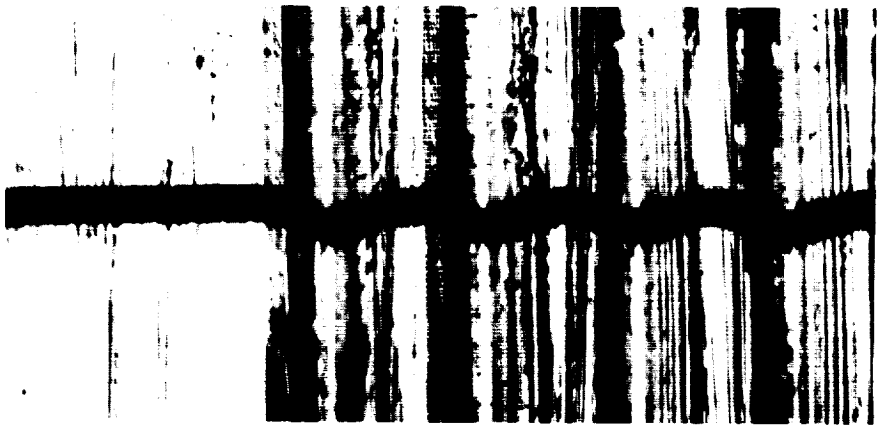

(c) Beginning of screwthread; thread depth 0.0003 inch; wire shadow; 514X.

Figure 5.- Photomicrographs of screwthreads on test models.

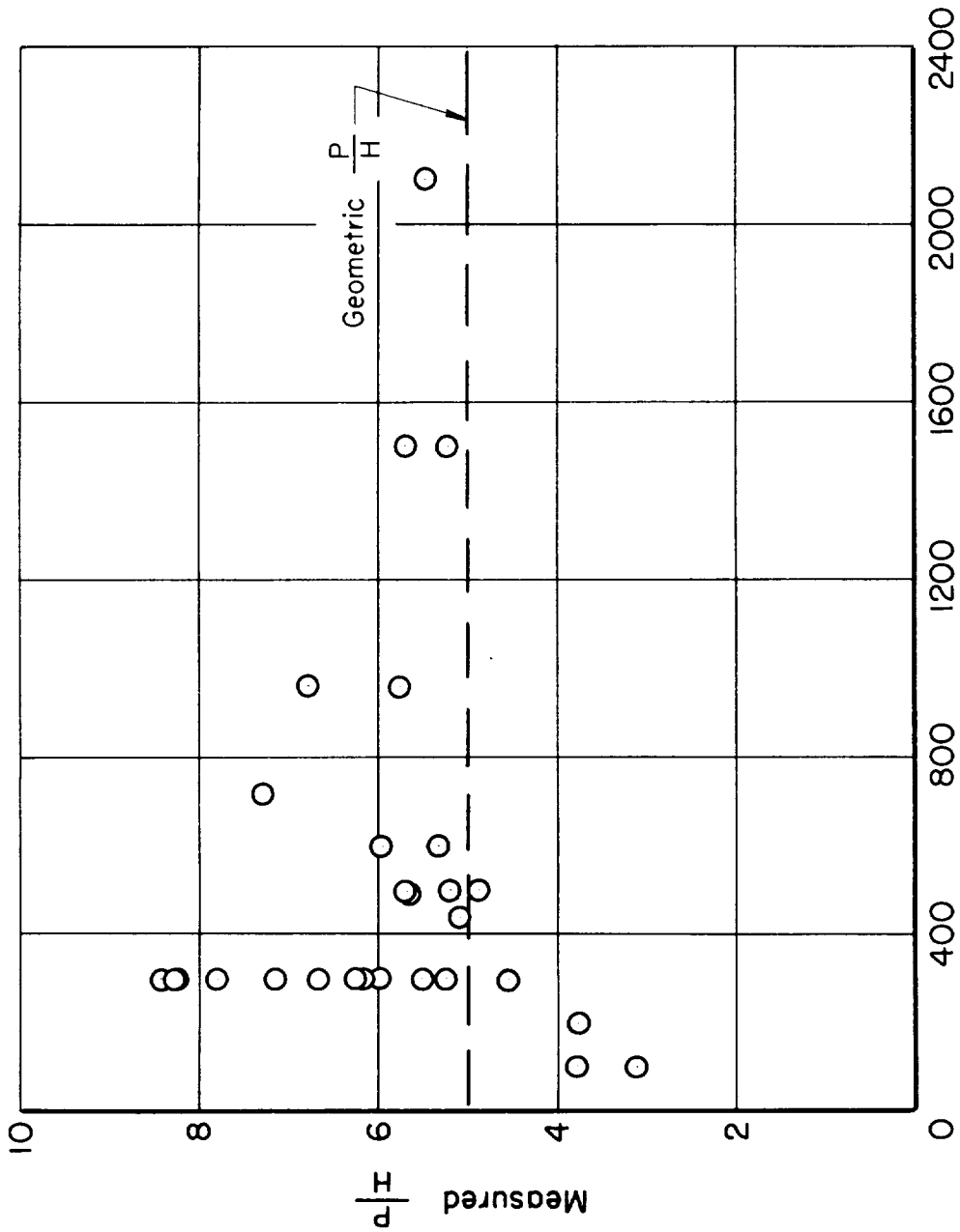

Figure 6.- Deviation of screwthread shapes from the geometric specification.

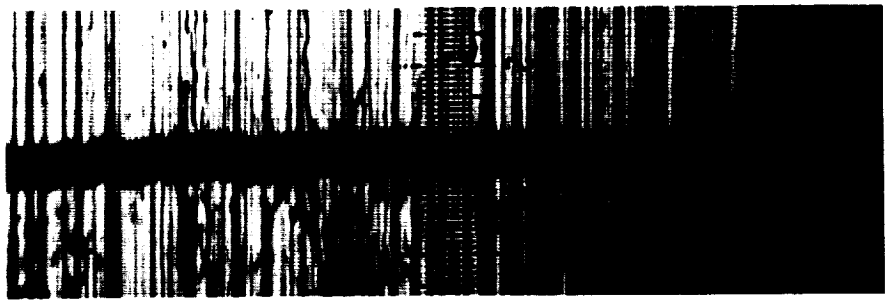

(a) 2/0 emery paper. Maximum scratch depth approximately 50 μin.; wire shadow; 1000X.

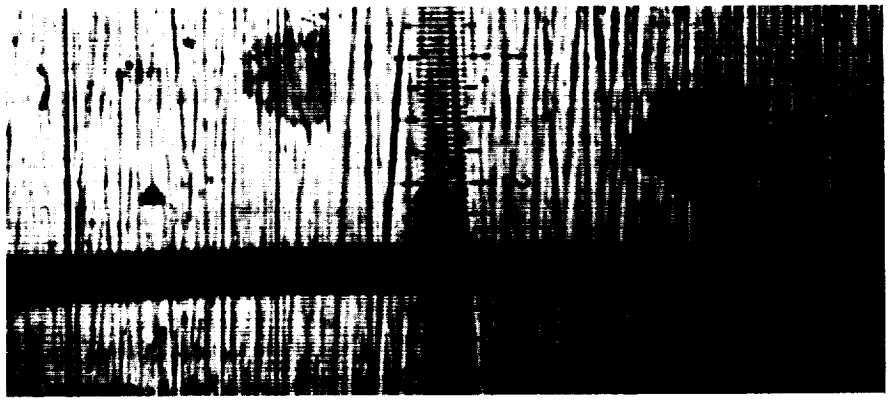

(b) 4/0 emery paper. Maximum scratch depth approximately 8 μin.; wire shadow; 1000X.

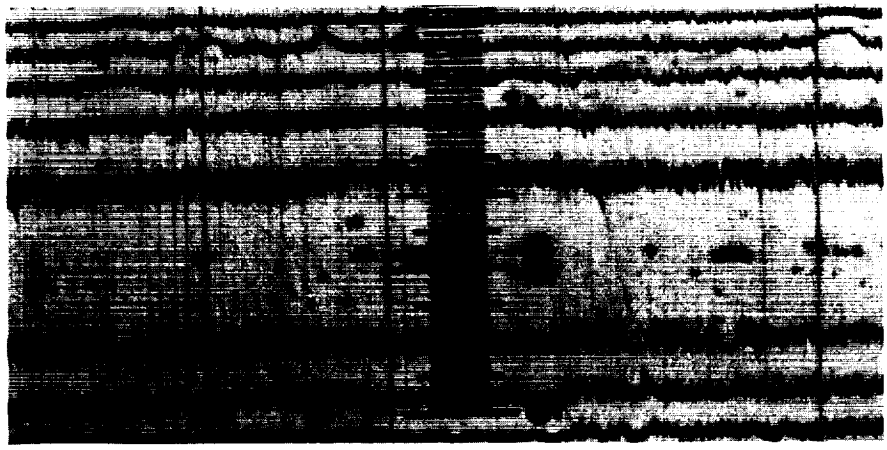

(c) 4/0 emery paper. Interferogram; fringe spacing = 10 μin.; 200X.

Figure 7.- Photomicrographs of scratch-polished surfaces on 7075-T6 alluminum alloy.

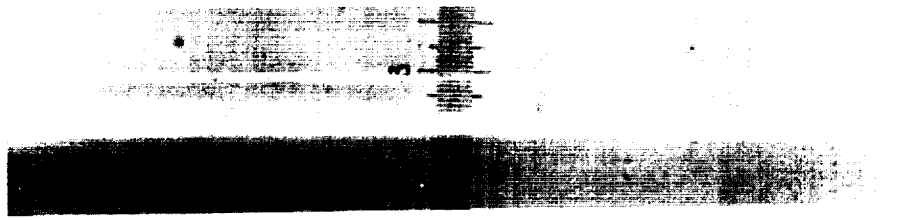

(a) Forward face of the leading edge of a contoured-tube model at maximum thickness; thickness = 0.00045 inch; 200X.

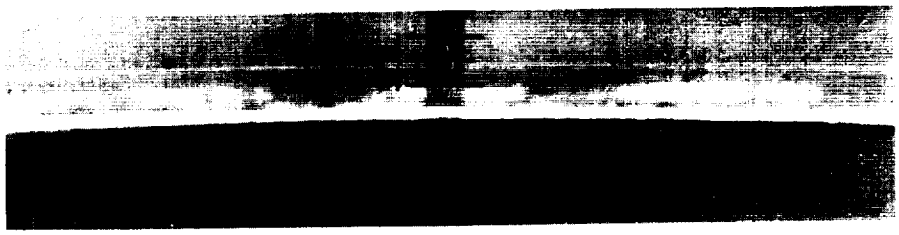

(b) Forward face of the leading edge of a contoured-tube model at minimum thickness; thickness = 0.0003 inch; 200X.

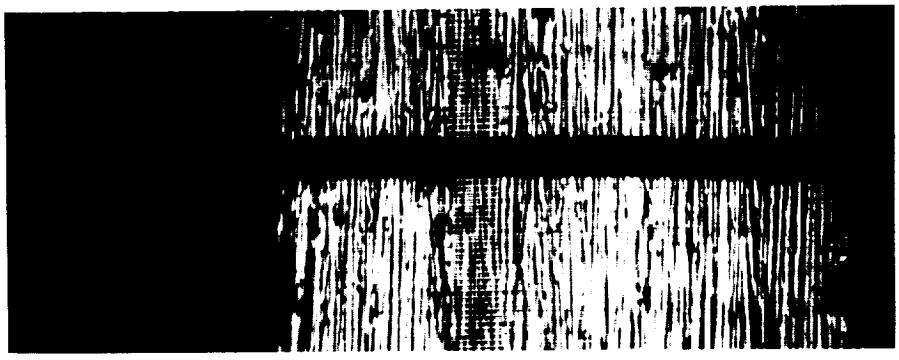

(c) Outer cylindrical surface of a straight-tube model at the leading edge; 2/0 finish; wire shadow; 514X.

Figure 8.- Photomicrographs of representative model leading edges.

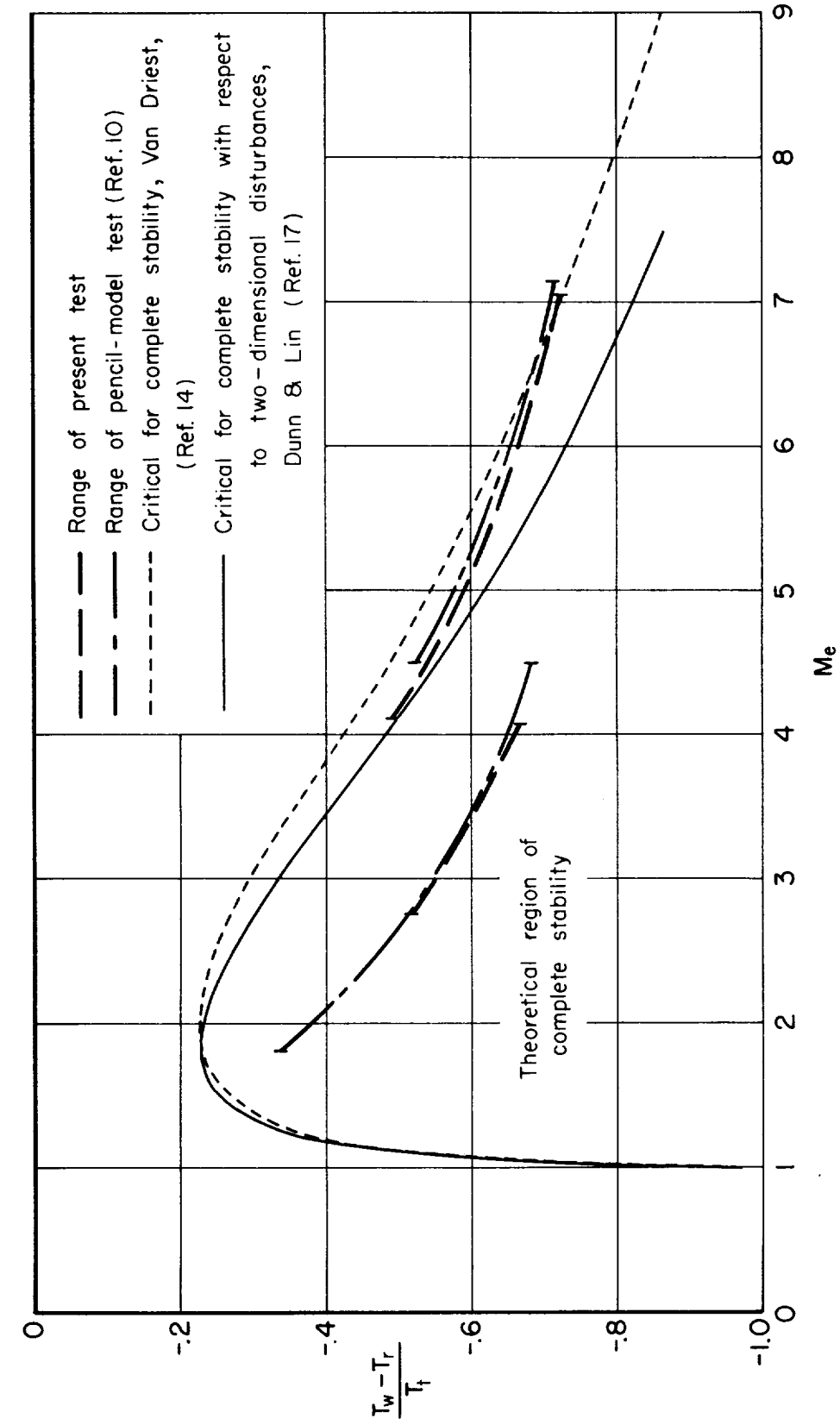

Figure 9.- Comparison of the temperature conditions of the present test to those of reference 10 and to the theoretical requirements for complete stability of the laminar boundary layer.

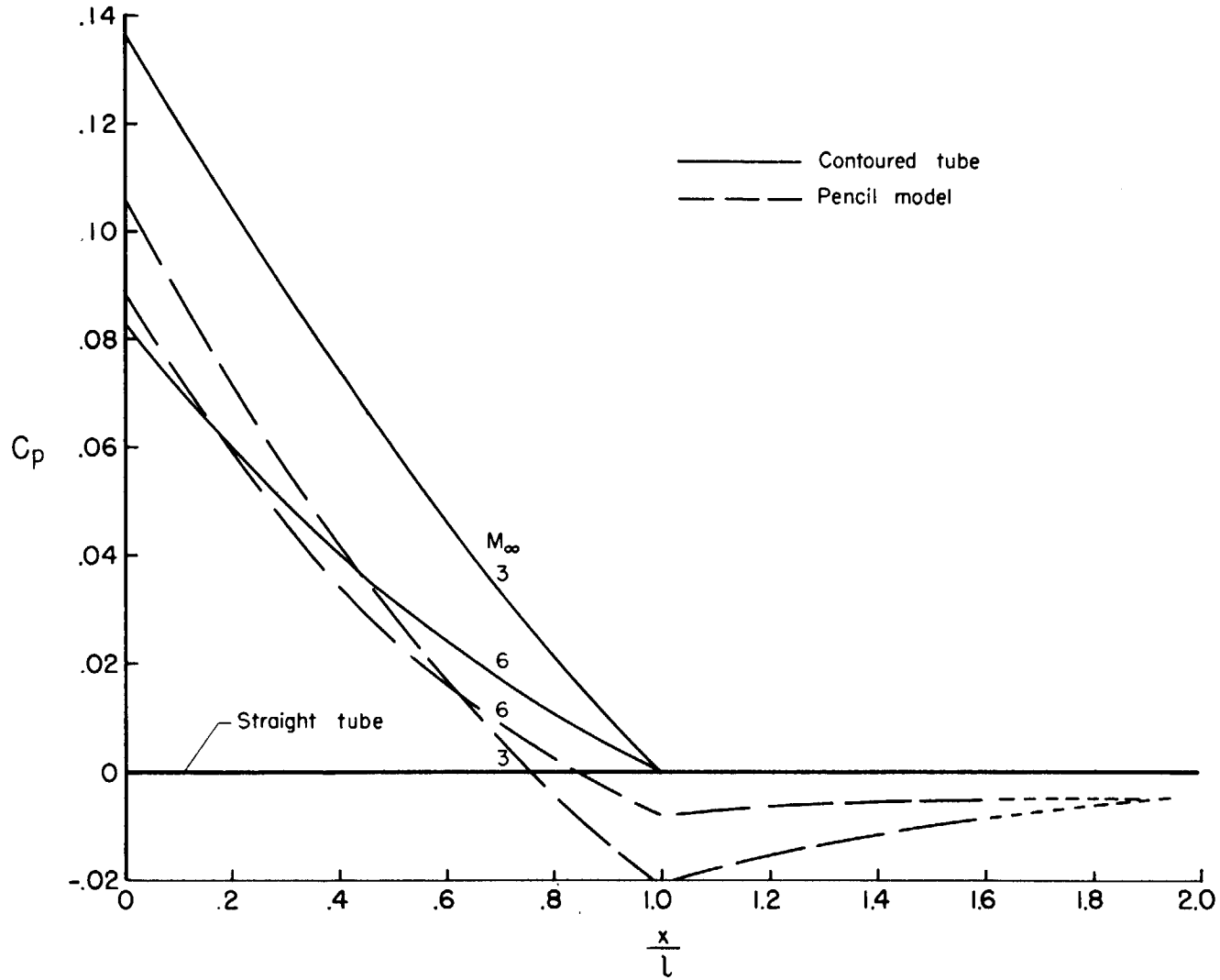

Figure 10.- Theoretical pressure distributions on the test models.

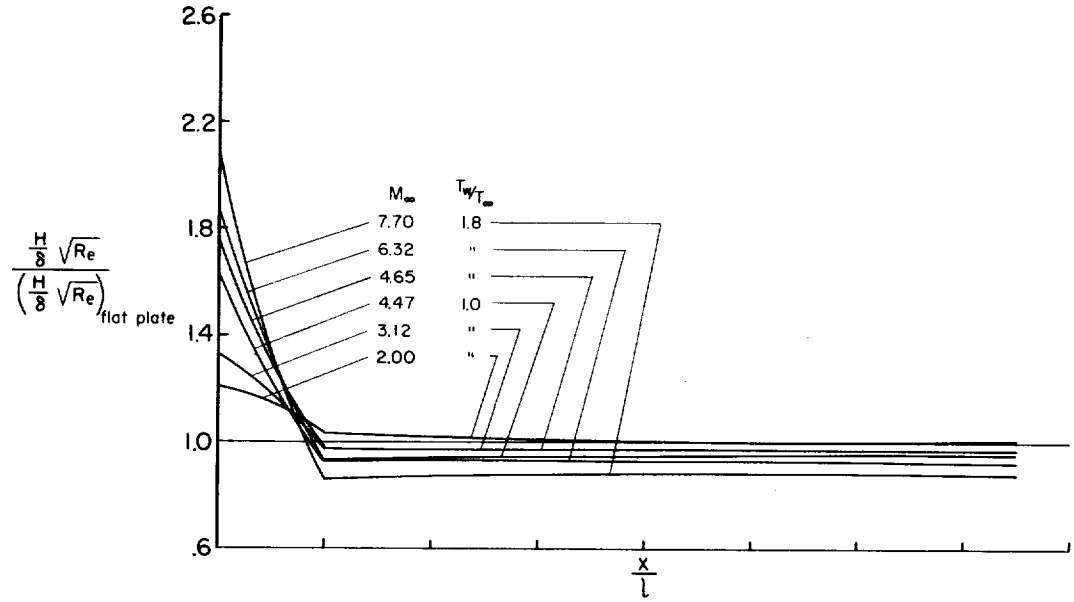

(a) Contoured tube.

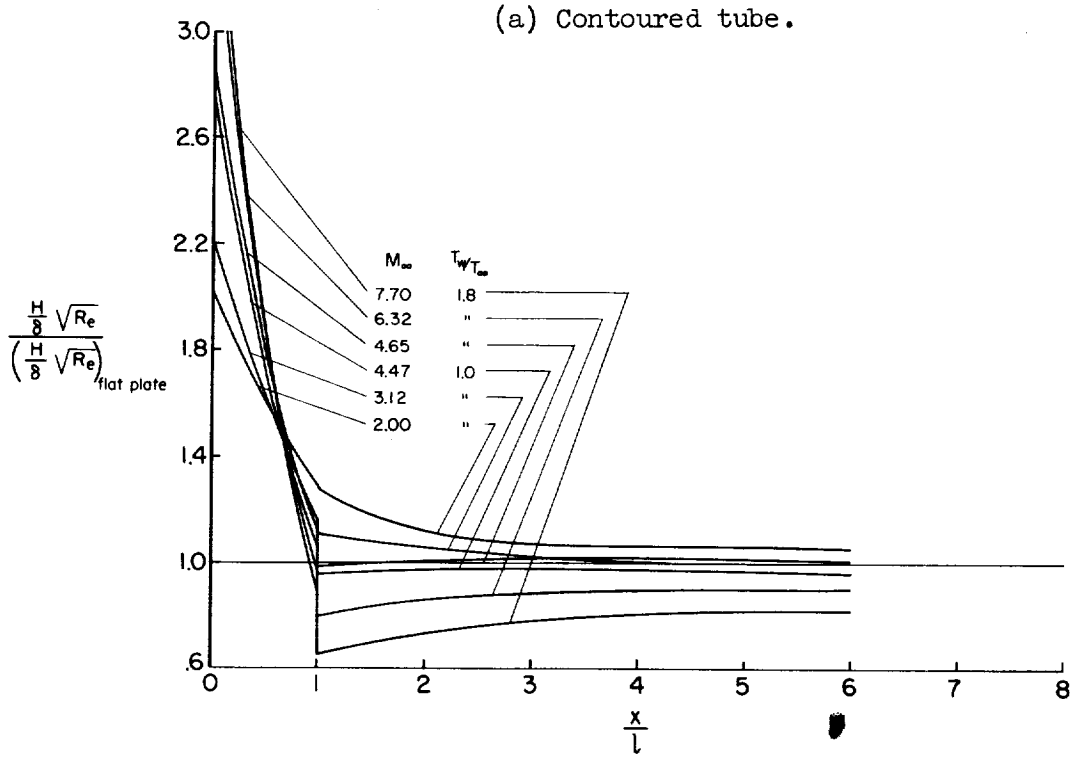

(b) Pencil model.

Figure 11.- Relative roughness of a given element on the contoured tube and pencil model compared to its roughness on a flat plate.

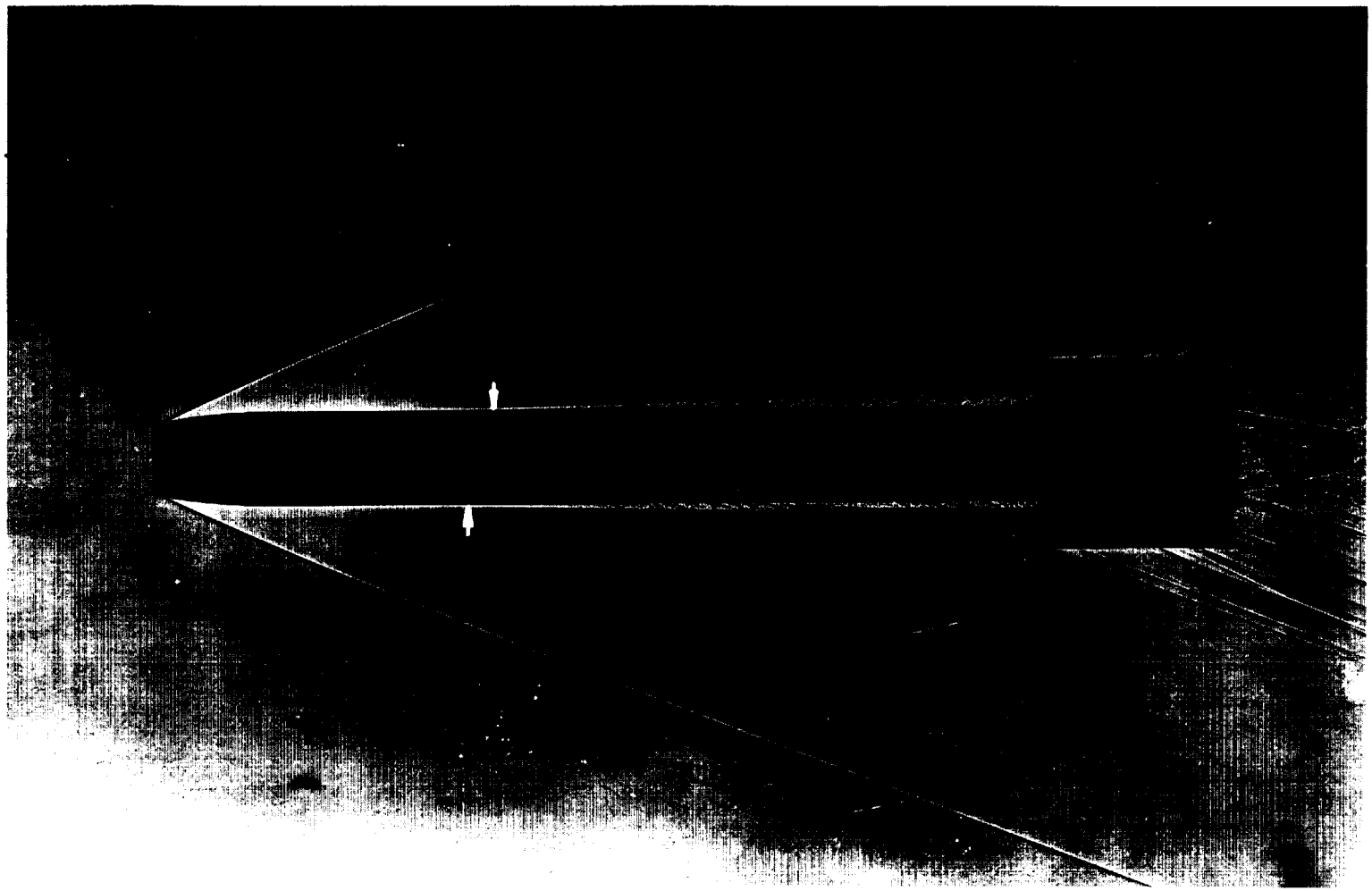

(a) Contoured tube; M_e = 3.1; screwthread finish; H ≈ 600 μin.

Figure 12.- Shadowgraphs of models in flight.

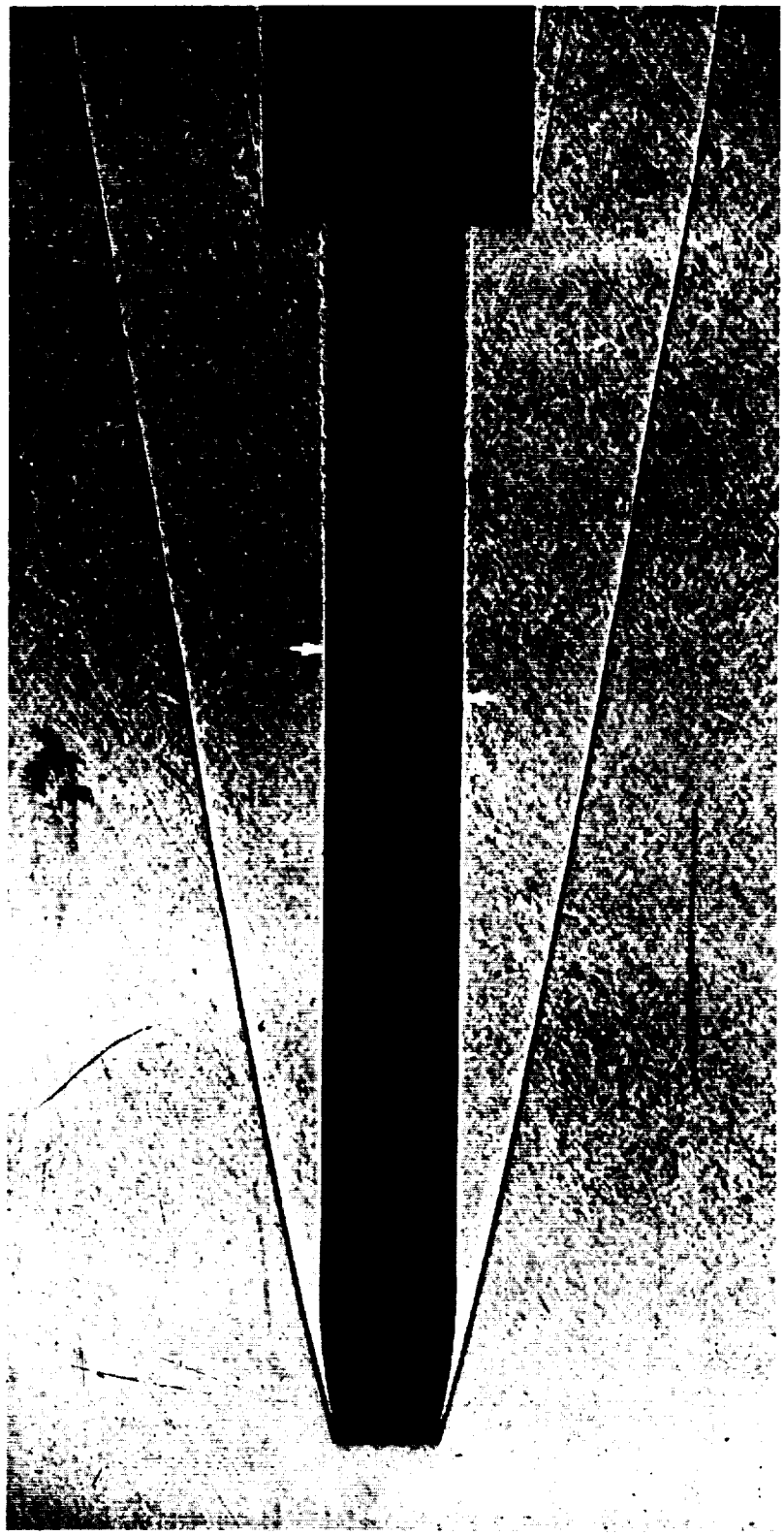

(b) Contoured tube; M_e = 7.1; screwthread finish; H ≈ 300 μin.

Figure 12.- Continued.

(c) Contoured tube; M_e = 7.0; screwthread finish; H ≈ 1500 μin.

Figure 12.- Continued.

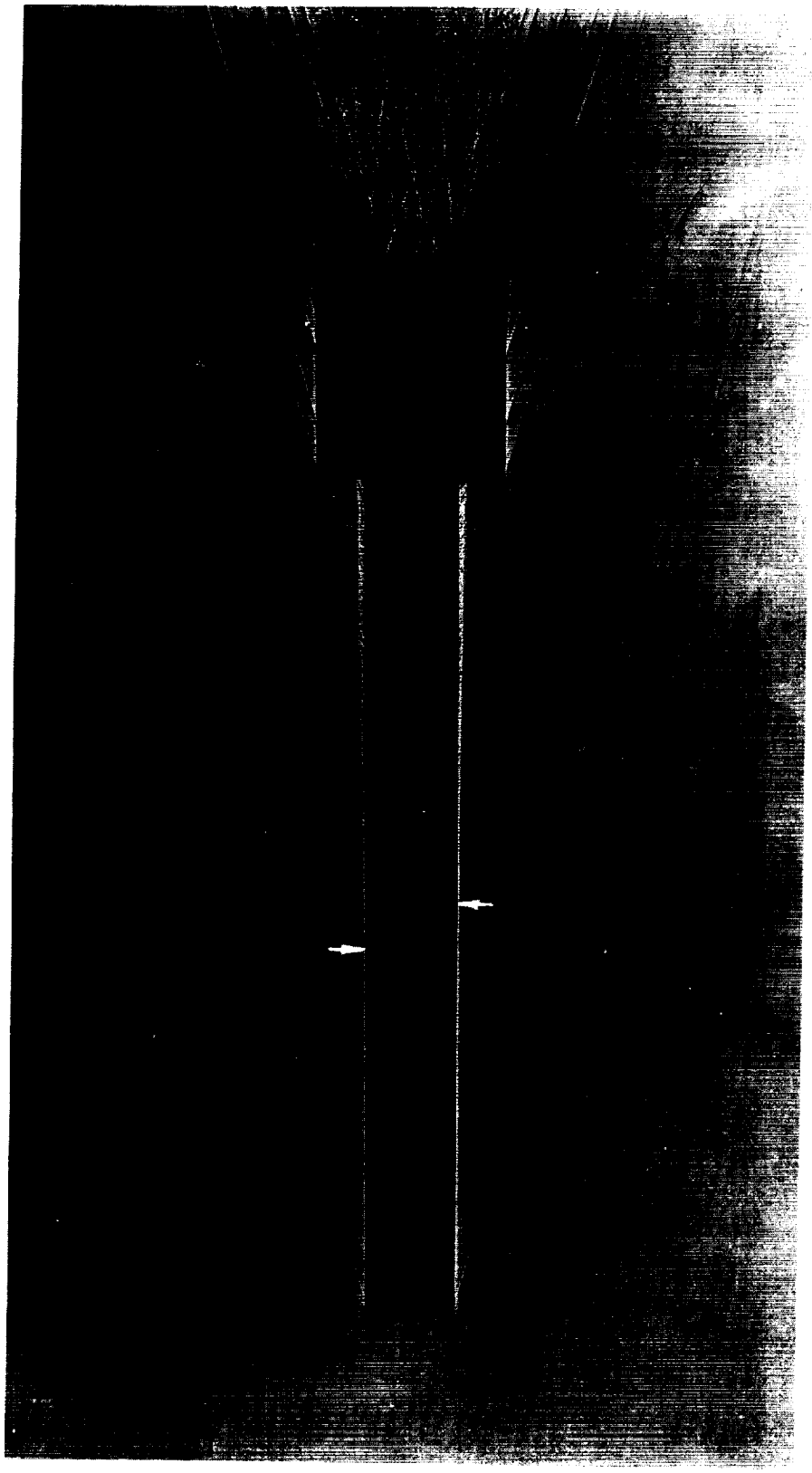

(d) Straight tube; M_e = 3.9; 2/0 finish; H ≈ 50 μin.

Figure 12.- Continued.

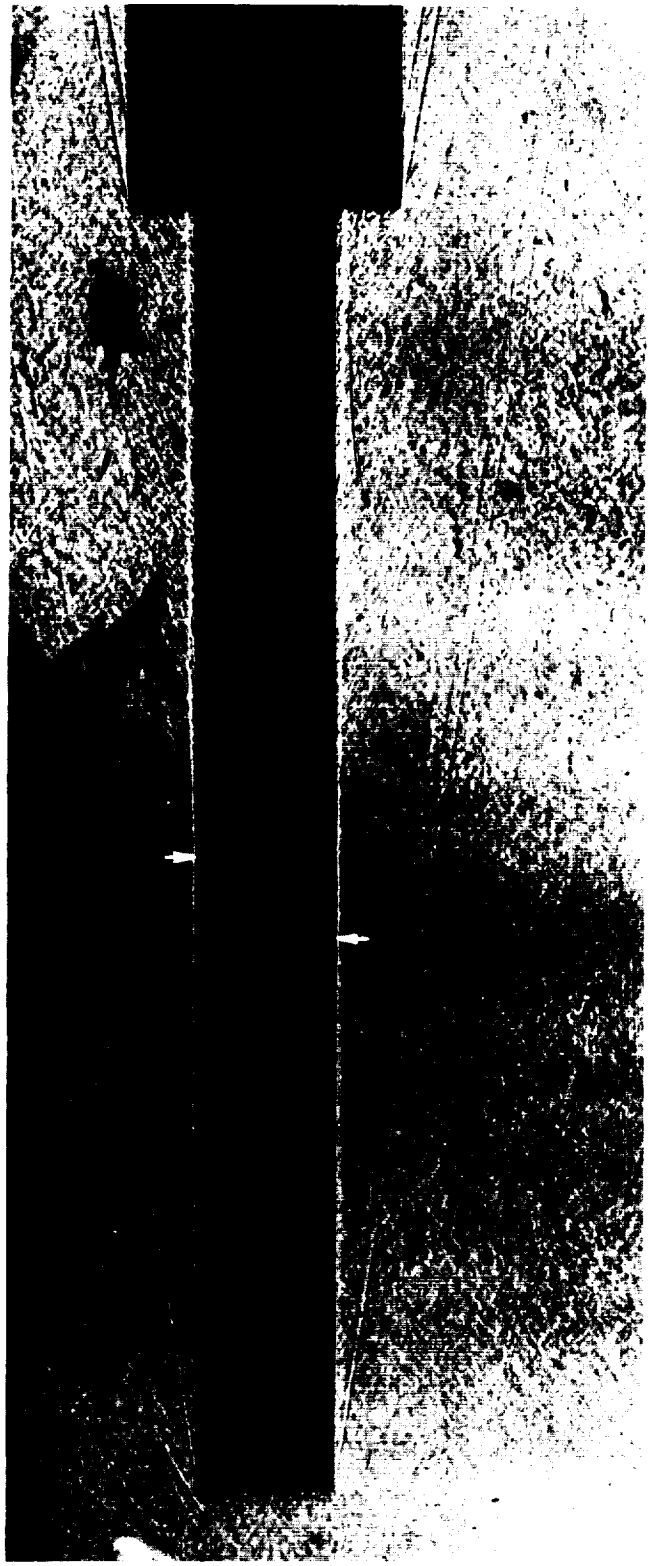

(e) Straight tube; M_e = 7.0; 4/0 finish; H ≈ 8 μin.

Figure 12.- Concluded.

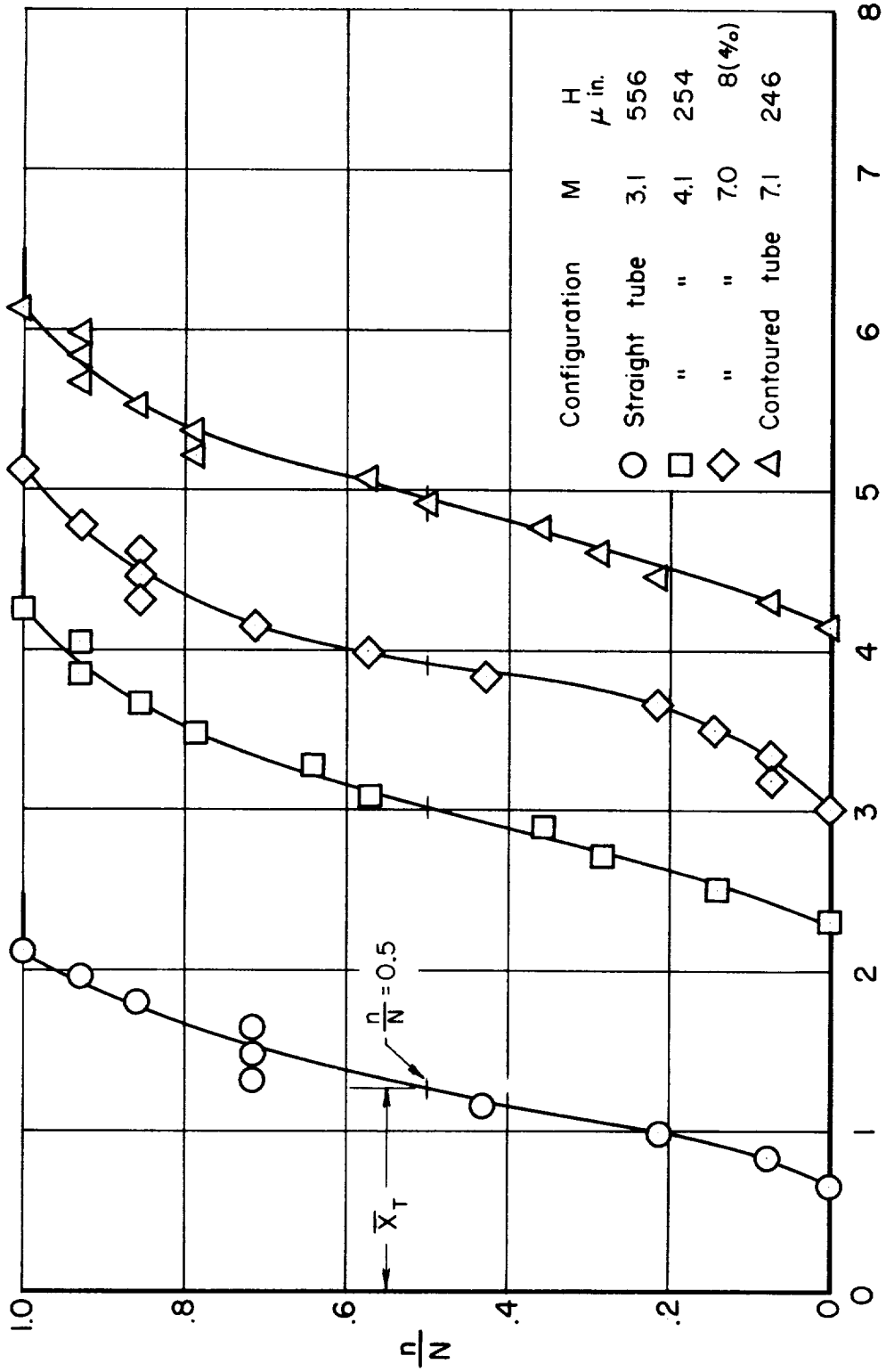

Figure 13.- Longitudinal distribution of the probability of turbulence for four typical model flights.

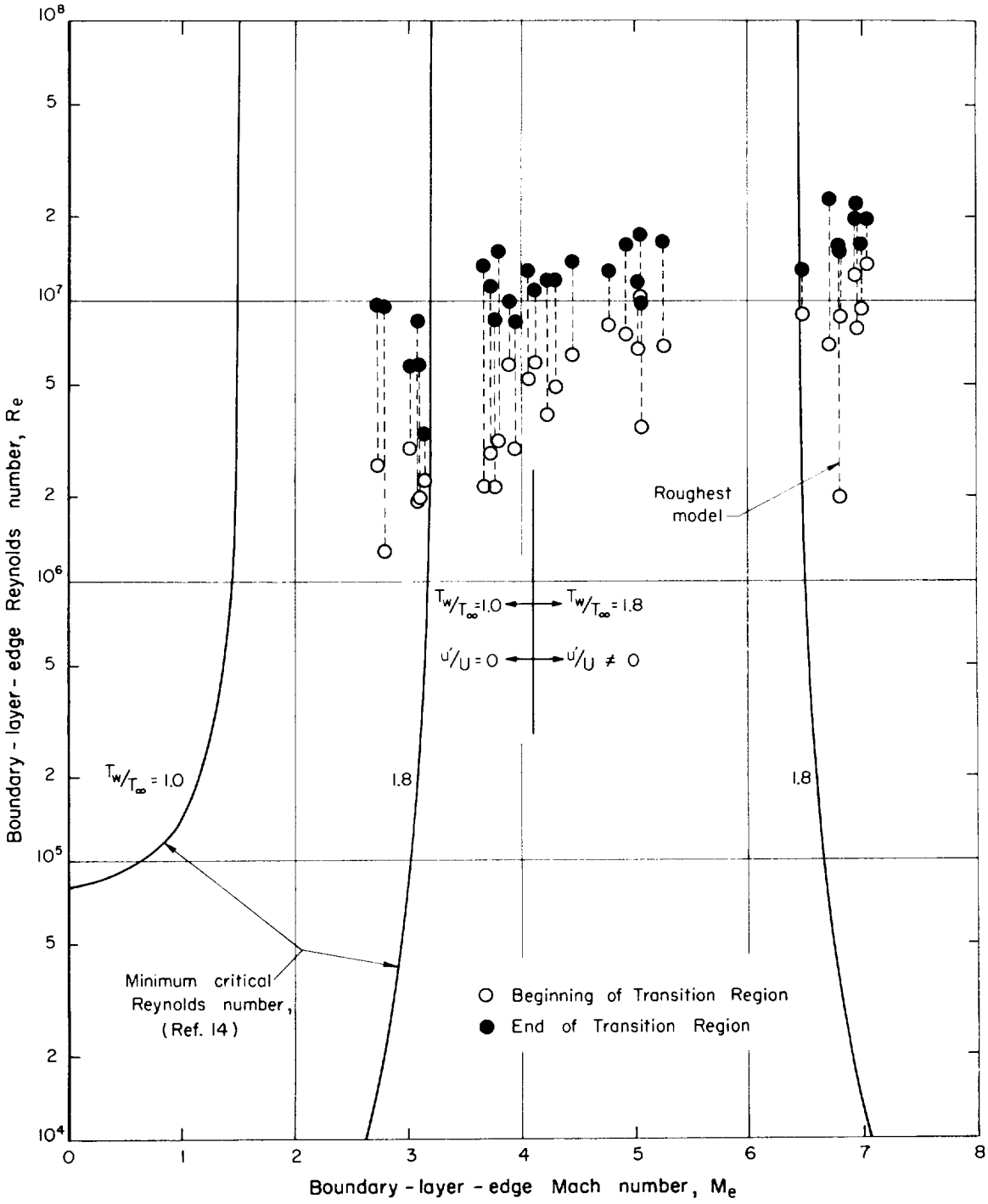

Figure 14.- Movement of the transition regions on the test models with variation of boundary-layer-edge Mach number.

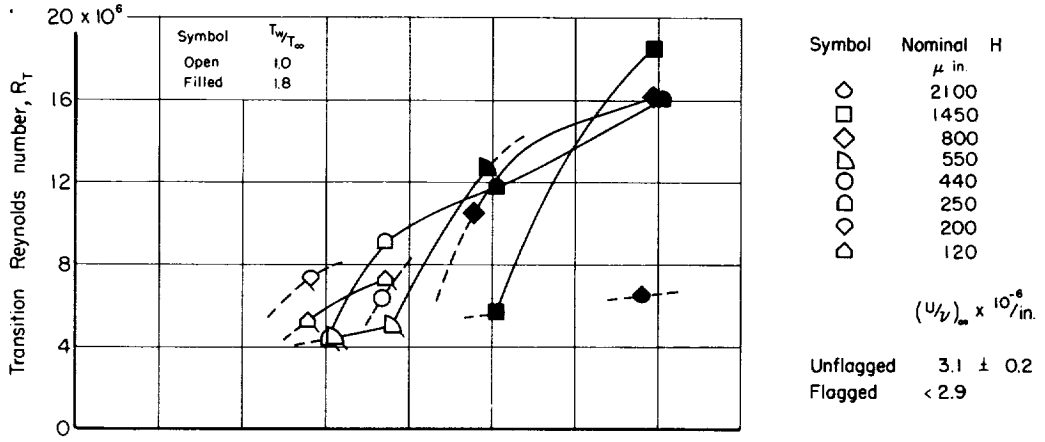

(a) Contoured tube.

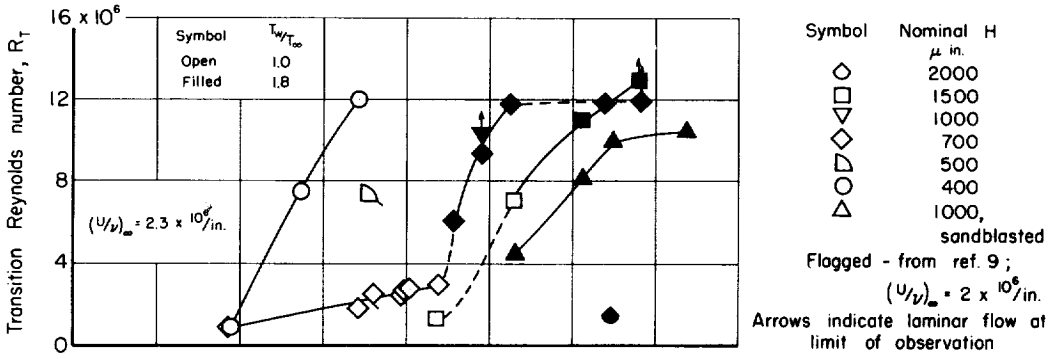

(b) Pencil model; Carros (ref. 10).

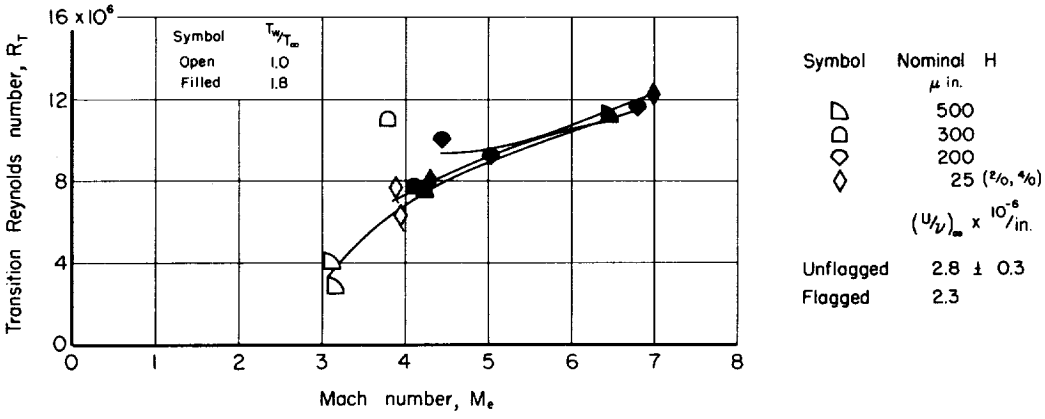

(c) Straight tube.

Figure 15.- Effect of Mach number variation on transition Reynolds number.

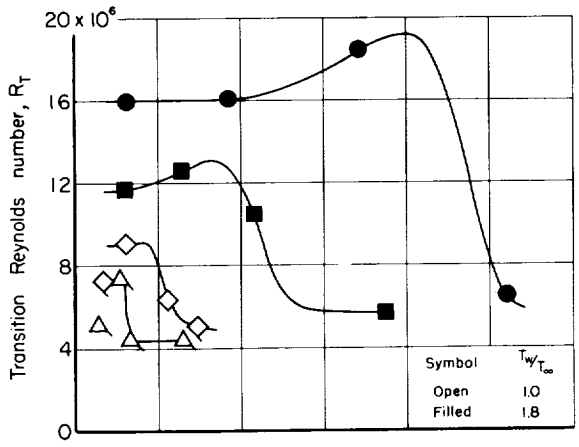

Symbol	Nominal M_e
○	7.0
□	5.0
◇	3.7
△	3.0

$(U/\nu)_\infty \times 10^{-6}$/in.

Unflagged	3.1 ± 0.2
Flagged	< 2.9

(a) Contoured tube.

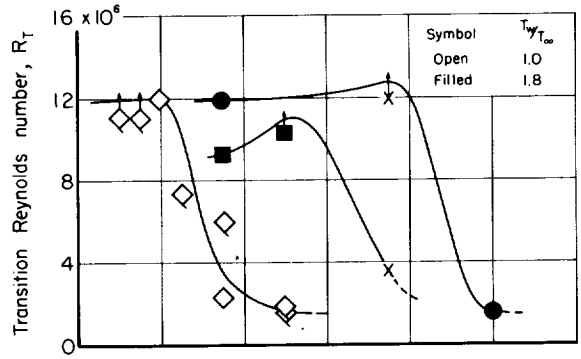

Symbol	Nominal M_e
○	6.4
□	4.9
◇	3.5
X	interpolated

	Ref.	$(U/\nu)_\infty \times 10^{-6}$/in.
Unflagged	10	2.3
Flagged	9	2.0

Arrows indicate laminar flow at limit of observation

(b) Pencil model.

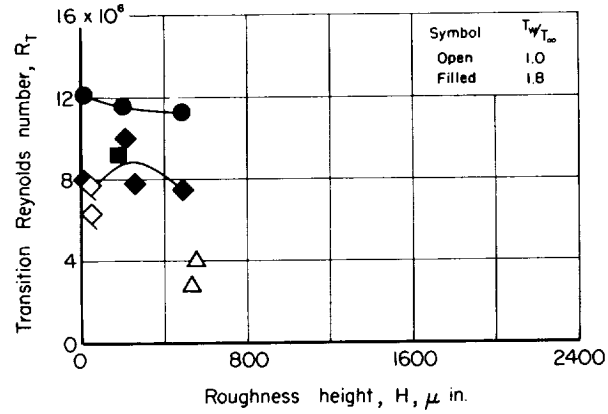

Symbol	Nominal M_e
○	6.8
□	5.0
◇	4.2
△	3.1

$(U/\nu)_\infty \times 10^{-6}$/in.

Unflagged	2.8 ± 0.3
Flagged	2.3

(c) Straight tube.

Figure 16.- Effect of roughness height variation on transition Reynolds number.

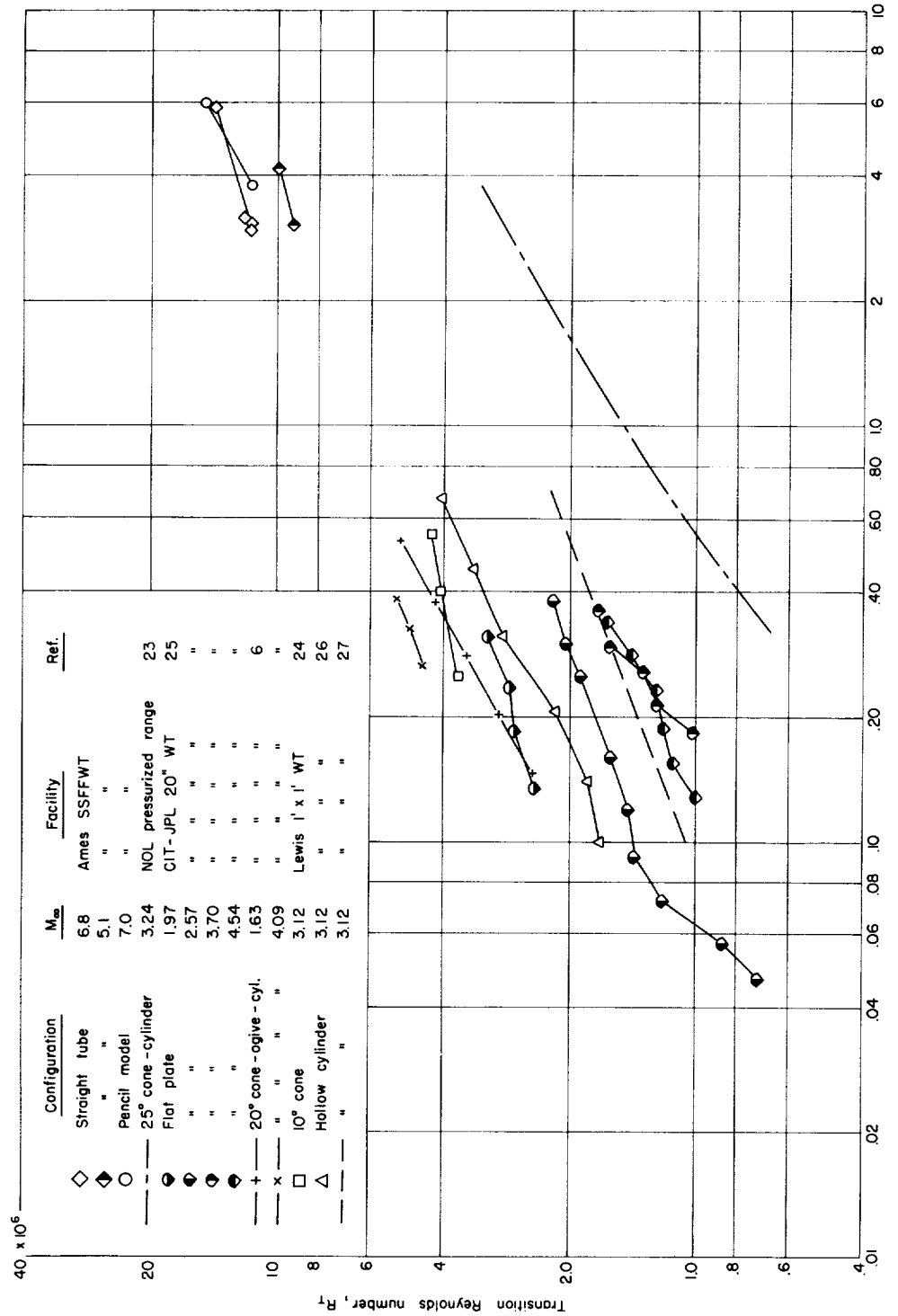

Figure 17.- Variation of transition Reynolds number with unit Reynolds number on surfaces having subcritical roughness.

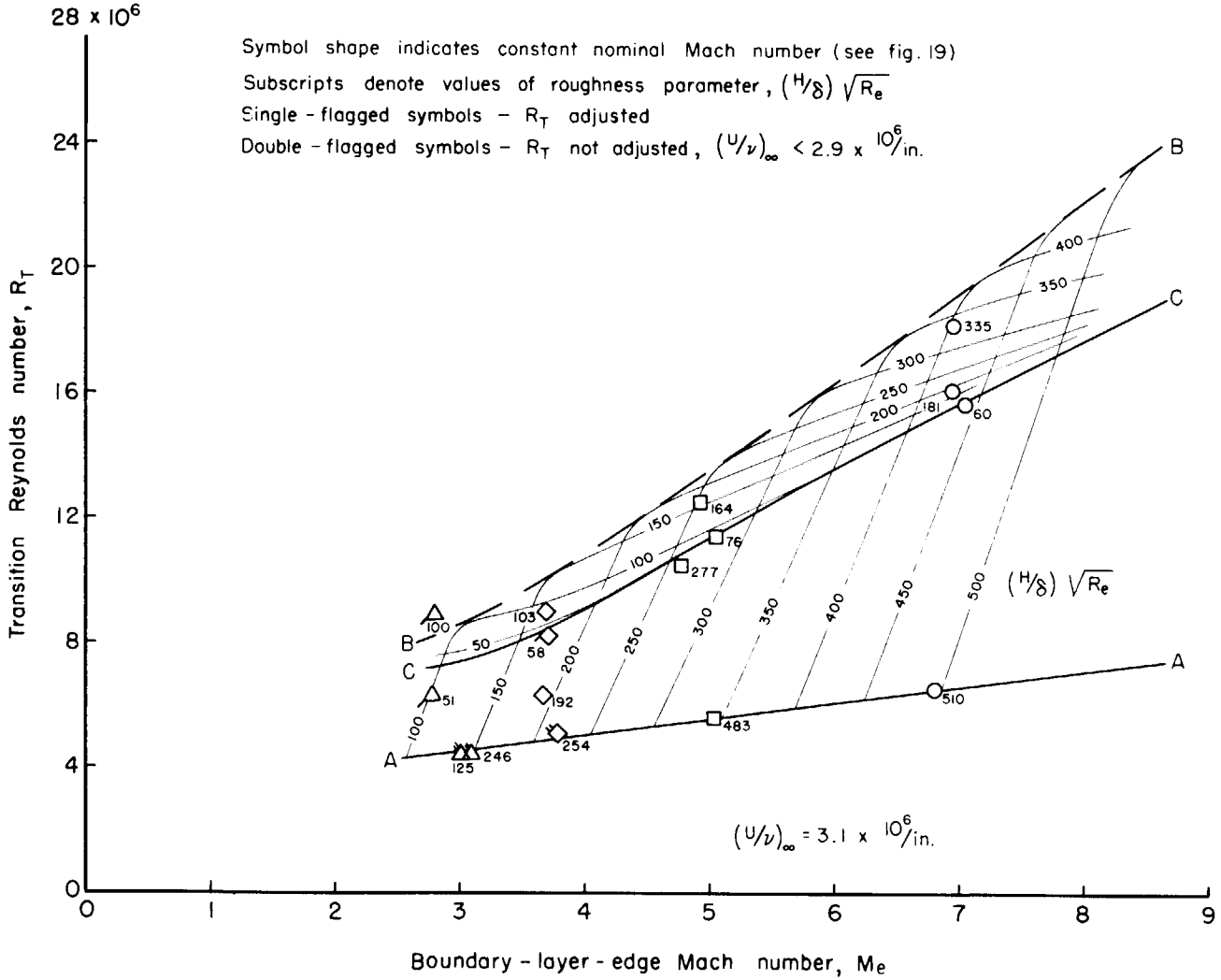

Figure 18.- Variation of transition Reynolds number with boundary-layer-edge Mach number for constant roughness parameter on the contoured tube.

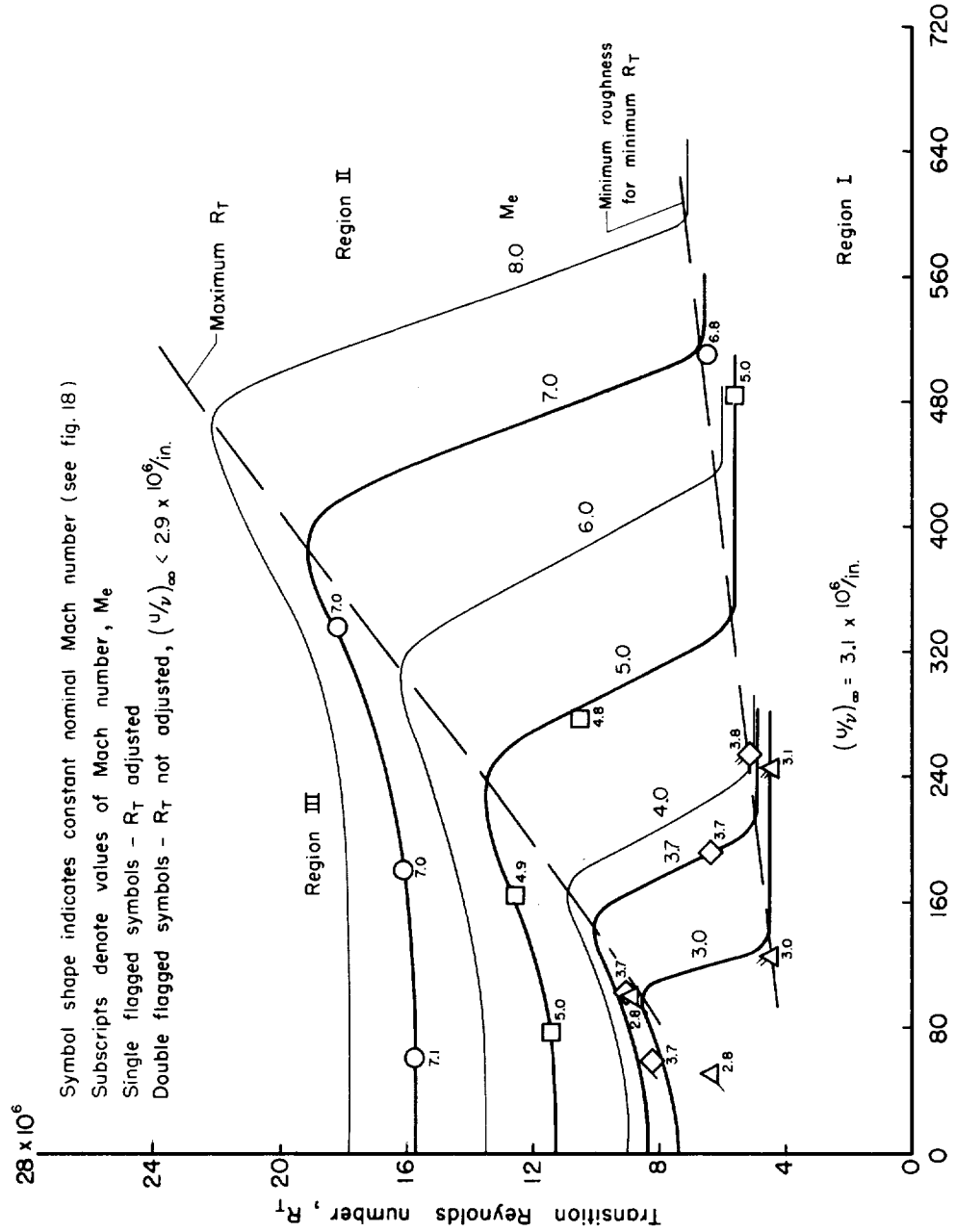

Figure 19.- Variation of transition Reynolds number with roughness parameter for constant boundary-layer-edge Mach number on the contoured tube.

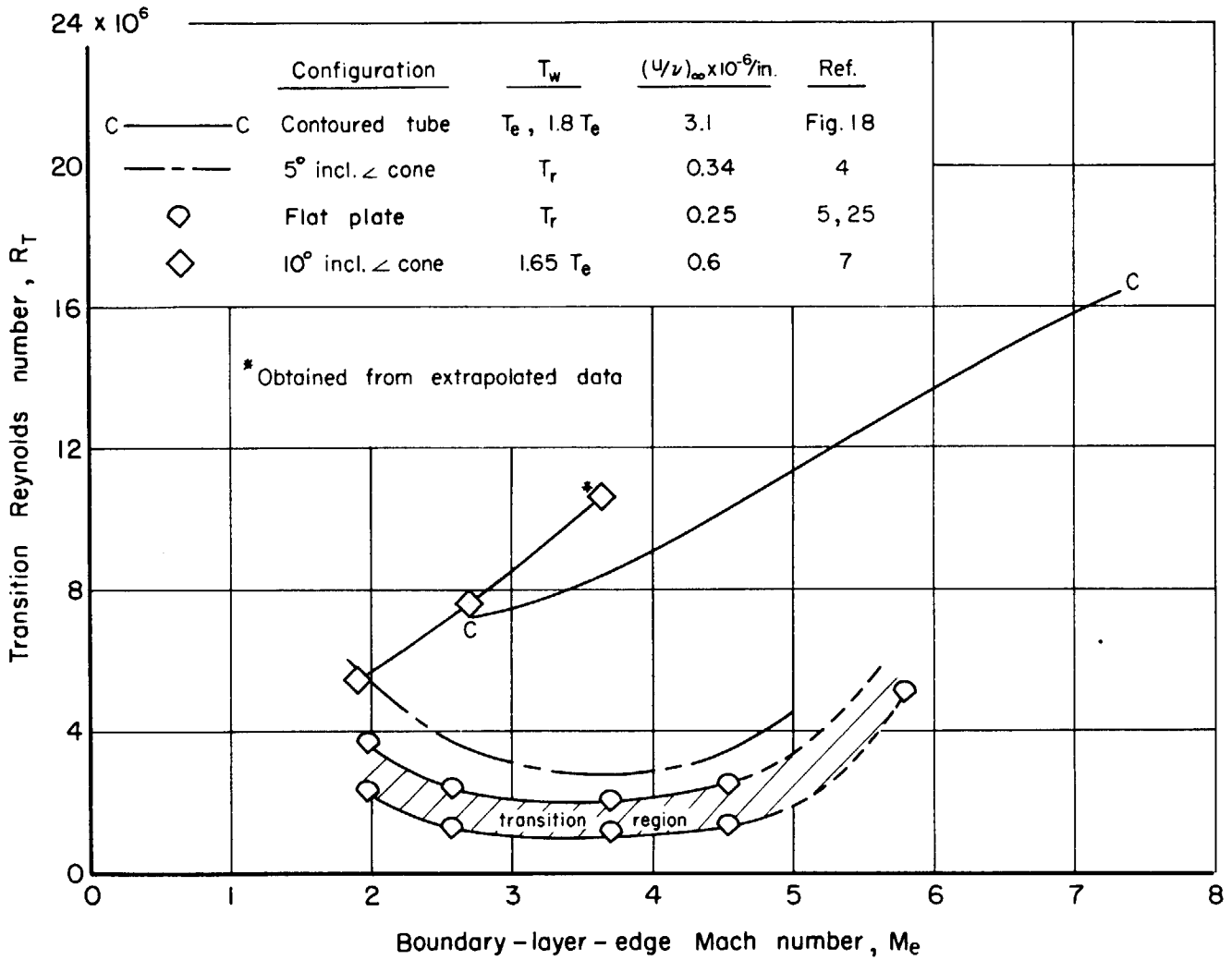

Figure 20.- Effect of Mach number on transition Reynolds number for two conditions of heat transfer; comparison of other data with present results for the contoured tube.

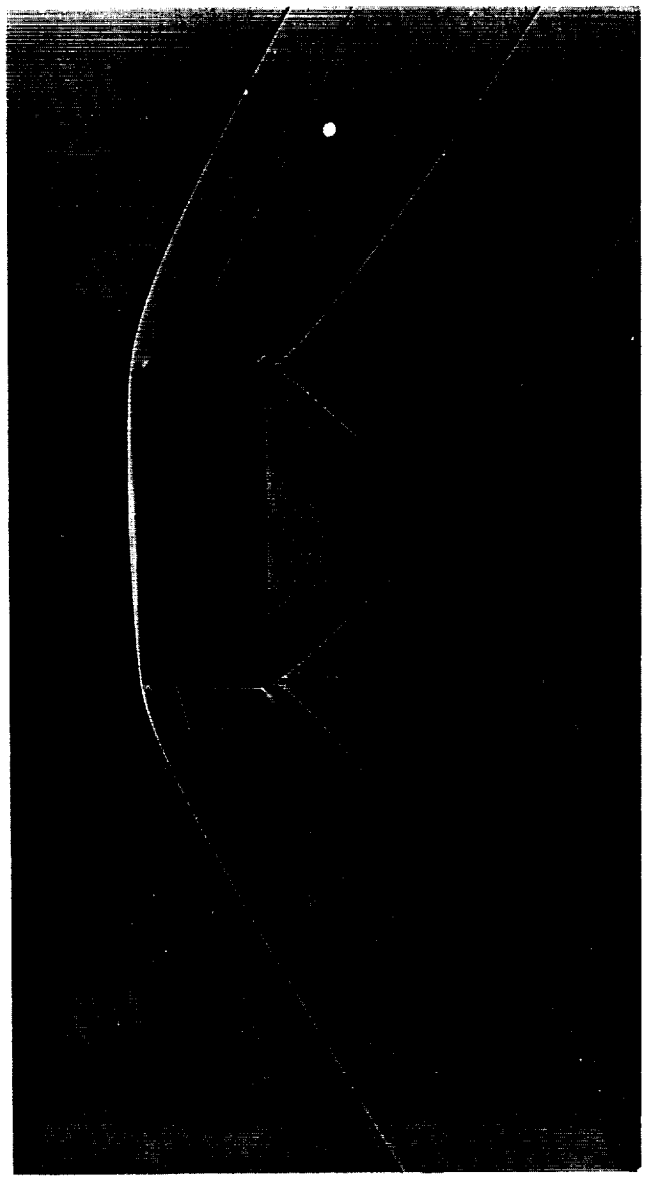

Figure 21.- Periodic pressure wavelets due to acoustic radiation from annular grooves cut in the outer surface of a short thin-walled hollow cylinder in free flight at Mach number 1.23.

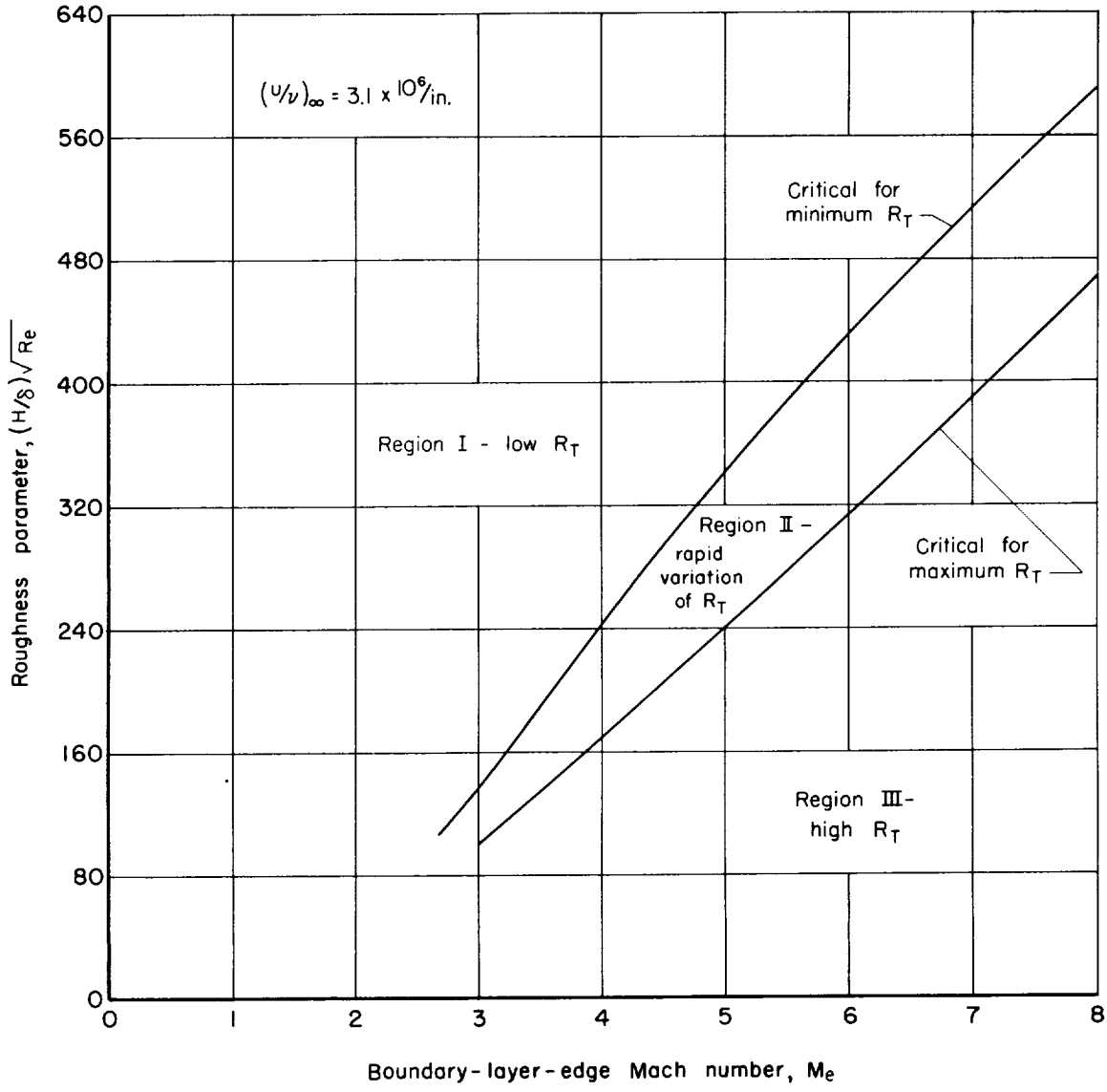

Figure 22.- Critical combinations of Mach number and roughness parameter for transition Reynolds number maximums and minimums on the contoured tube.

NASA MEMO 1-20-59A
National Aeronautics and Space Administration.
BOUNDARY-LAYER TRANSITION ON HOLLOW CYLINDERS IN SUPERSONIC FREE FLIGHT AS AFFECTED BY MACH NUMBER AND A SCREW-THREAD TYPE OF SURFACE ROUGHNESS.
Carlton S. James. February 1959. 49p. diagrs., photos. (NASA MEMORANDUM 1-20-59A)

Test Mach numbers were between 2.8 and 7 with a unit Reynolds number of 3 million per inch. Model surfaces were cold relative to stagnation temperatures. Transition Reynolds number was found to increase with Mach number throughout the range tested. Roughness required to influence transition increased with Mach number. Certain optimum roughnesses were found which permitted longer laminar runs than did a smooth surface.

Copies obtainable from NASA, Washington

1. Flow, Supersonic (1.1.2.3)
2. Flow, Laminar (1.1.3.1)
3. Flow, Turbulent (1.1.3.2)
4. Bodies - Surface Conditions (1.3.2.4)

I. James, Carlton S.
II. NASA MEMO 1-20-59A

NASA

NASA MEMO 1-20-59A
National Aeronautics and Space Administration.
BOUNDARY-LAYER TRANSITION ON HOLLOW CYLINDERS IN SUPERSONIC FREE FLIGHT AS AFFECTED BY MACH NUMBER AND A SCREW-THREAD TYPE OF SURFACE ROUGHNESS.
Carlton S. James. February 1959. 49p. diagrs., photos. (NASA MEMORANDUM 1-20-59A)

Test Mach numbers were between 2.8 and 7 with a unit Reynolds number of 3 million per inch. Model surfaces were cold relative to stagnation temperatures. Transition Reynolds number was found to increase with Mach number throughout the range tested. Roughness required to influence transition increased with Mach number. Certain optimum roughnesses were found which permitted longer laminar runs than did a smooth surface.

Copies obtainable from NASA, Washington

1. Flow, Supersonic (1.1.2.3)
2. Flow, Laminar (1.1.3.1)
3. Flow, Turbulent (1.1.3.2)
4. Bodies - Surface Conditions (1.3.2.4)

I. James, Carlton S.
II. NASA MEMO 1-20-59A

NASA

NASA MEMO 1-20-59A
National Aeronautics and Space Administration.
BOUNDARY-LAYER TRANSITION ON HOLLOW CYLINDERS IN SUPERSONIC FREE FLIGHT AS AFFECTED BY MACH NUMBER AND A SCREW-THREAD TYPE OF SURFACE ROUGHNESS.
Carlton S. James. February 1959. 49p. diagrs., photos. (NASA MEMORANDUM 1-20-59A)

Test Mach numbers were between 2.8 and 7 with a unit Reynolds number of 3 million per inch. Model surfaces were cold relative to stagnation temperatures. Transition Reynolds number was found to increase with Mach number throughout the range tested. Roughness required to influence transition increased with Mach number. Certain optimum roughnesses were found which permitted longer laminar runs than did a smooth surface.

Copies obtainable from NASA, Washington

1. Flow, Supersonic (1.1.2.3)
2. Flow, Laminar (1.1.3.1)
3. Flow, Turbulent (1.1.3.2)
4. Bodies - Surface Conditions (1.3.2.4)

I. James, Carlton S.
II. NASA MEMO 1-20-59A

NASA

NASA MEMO 1-20-59A
National Aeronautics and Space Administration.
BOUNDARY-LAYER TRANSITION ON HOLLOW CYLINDERS IN SUPERSONIC FREE FLIGHT AS AFFECTED BY MACH NUMBER AND A SCREW-THREAD TYPE OF SURFACE ROUGHNESS.
Carlton S. James. February 1959. 49p. diagrs., photos. (NASA MEMORANDUM 1-20-59A)

Test Mach numbers were between 2.8 and 7 with a unit Reynolds number of 3 million per inch. Model surfaces were cold relative to stagnation temperatures. Transition Reynolds number was found to increase with Mach number throughout the range tested. Roughness required to influence transition increased with Mach number. Certain optimum roughnesses were found which permitted longer laminar runs than did a smooth surface.

Copies obtainable from NASA, Washington

1. Flow, Supersonic (1.1.2.3)
2. Flow, Laminar (1.1.3.1)
3. Flow, Turbulent (1.1.3.2)
4. Bodies - Surface Conditions (1.3.2.4)

I. James, Carlton S.
II. NASA MEMO 1-20-59A

NASA